Czech Technical University in Prague
Faculty of Nuclear Sciences and Physical Engineering

DOCTORAL THESIS

State Transfer in Imperfect Networks

Prague 2020 Antonín Hoskovec

Bibliografický záznam:

Autor:	Ing. Antonín Hoskovec České vysoké učení technické v Praze Fakulta jaderná a fyzikálně inženýrská Katedra fyziky
Název práce:	Přenos stavu na sítích s poruchou
Studijní program:	Matematické inženýrství
Studijní obor:	Matematická fyzika
Školitel:	prof. Ing. Igor Jex, DrSc. České vysoké učení technické v Praze Fakulta jaderná a fyzikálně inženýrská Katedra fyziky
Akademický rok:	2019/2020
Počet stran:	89
Klíčová slova:	přenos kvantového stavu, kvantové korekční algoritmy, kvantové sítě

Bibliographic Entry:

Author:	Ing. Antonín Hoskovec Czech Technical University in Prague Faculty of Nuclear Sciences and Physical Engineering Department of Physics
Title of Dissertation:	State Transfer in Imperfect Networks
Degree Programme:	Mathematical Engineering
Field of Study:	Mathematical Physics
Supervisor:	prof. Ing. Igor Jex, DrSc. Czech Technical University in Prague Faculty of Nuclear Sciences and Physical Engineering Department of Physics
Academic Year:	2019/2020
Number of Pages:	89
Keywords:	quantum state transfer, quantum correction algorithms, quantum networks

Acknowledgment

My path to writing my doctoral thesis (which is now in your hands) was not a straight one. Through the best and worst of it I consider myself lucky to have had the support of my supervisor Professor Igor Jex, the leader of our faculty. He just might be the most kind, understanding and brilliant person you will ever meet.

Working on the topics related to Quantum State Transfer has allowed me to meet many great people. I have learned most of what I know about Dynamical Decoupling from Dr. Holger Frydrych and the group of Professor Gernot Alber in Darmstadt. Dr. Georgios M. Nikolopoulos was the one to introduce me to Quantum Optics and realistic considerations about the idealized physical models after he kindly invited me to work with him in Crete.

The doctoral studies were a bittersweet experience. On one hand I loved the challenges, the time I spent with my colleagues and friends, the traveling. On the other, it took me longer than it should have to get here. I would not have made it had I not been able to rely on my loving family. I do not think I will ever understand how my wife, my mother and my sister have only shown kindness towards the likes of me during it all.

To all of you, from the bottom of my heart, thank you.

Abstrakt: Věrný přenos kvantového stavu je jedním ze stavebních kamenů kvantového počítače. Jelikož se jedná o unitární transformaci, je proveditelný na jakémkoliv kvantovém počítači. Při použití konvenčních procedur, které spoléhají na sekvenční aplikaci elementárních unitárních transformací (např. SWAP operací), dochází často ke kvantové dekoherenci systému. Namísto toho existují metody, které navrhnou interakce mezi částmi kvantové sítě tak, aby k přenosu stavu došlo bez jakékoliv vnější kontroly. Existují experimentální výsledky potvrzující výhody takového přístupu. Reálné fyzikální systémy se vždy odchylují od idealizovaných modelů, které používáme k jejich popisu, a tak i systémy určené k pasivnímu přenosu stavu mohou trpět nedostatky. Ukážeme závažné důsledky několika poruch inspirovaných fyzikální podstatou takových systémů. K opravě těchto poruch navrhujeme uvolnit požadavek minimální kontroly natolik, aby se dala použít kvantová korekční metoda Dynamical decoupling. Při této metodě se omezíme na použití jednočásticových operací. Nalezli jsme řadu Dynamical decoupling schémat, které poruchy efektivně odstraňují. Jejich funkčnost jsme ověřili numerickými simulacemi.

Abstract: Reliable method of quantum state transfer is one of the fundamental requirements of building a quantum computer. It is a unitary transformation, hence it is achievable on any quantum computer. However, when using conventional methods of sequential applications of elementary unitary transformations (such as the SWAP operations), quantum decoherence often becomes an issue. Instead there are methods of designing the interactions between various parts of the quantum network such that quantum state transfer occurs with no external control whatsoever. There are recent experimental results supporting the efficiency of these methods. Real world systems always deviate from their idealized models, quantum state transfer networks being no exception. We explore the adverse effects of several perturbations of the ideal models inspired by the physical character of these systems. To correct for the occurring errors we propose to relax the requirement of no external control enough that Dynamical Decoupling, a quantum error correction method, becomes applicable. This method is restricted to using single-particle operations only. We found several Dynamical Decoupling schemes which efficiently eliminate the errors from the network. We verified their performance with numerical simulations.

Contents

Chapter 1

Opening Remarks

Research in the field of Quantum Physics has branched and grown significantly since the construction of the first laser by Theodore H. Maiman in 1960. While originally the focus was primarily on the fundamental aspects of the theory, new branches such as Quantum Information Processing have attracted more and more attention. The pace of research in these new areas has been accelerating with the use of new unfamiliar phenomena for Quantum Computing as well as Quantum Communication. The ambition is to put the theory to practice i.e. to have quantum based computation, many of the proposed experiments have already been successfully demonstrated. The first crucial steps, however spectacular, do not guarantee overall success. Issues of scaling up the system, long coherence times etc. are the issues of the day. Finding new, more effective methods of engineering, controlling and protecting quantum systems now becomes imperative.

Quantum State Transfer (QST) is an example of streamlining some of the basic operations used in quantum computers. It is one of the cornerstones of building a large quantum computer since the main focus of a quantum computer should be on following the various quantum algorithms and the resources it has are limited [1]. Therefore minimal resources should be spent on the preparation and transport of the input state, reading from and writing to memory and even communication between different quantum computers. As a task QST can be achieved on any universal quantum computer since it is seemingly one of the simpler yet nontrivial unitary operations. However, relying on various decompositions of QST into elementary operations such as sequential SWAP gates can hinder the performance of a quantum computer, extend the computation times and introduce decoherence [1]. More efficient methods that achieve it have therefore been described over the years [2, 3, 4].

QST is intimately linked to excitation transfer, communication between remote sites

and remote entanglement creation [1]. Essentially it is the task of placing an arbitrary, unknown quantum state to a predefined location in a quantum network at a well defined moment in time from a given input position. In dependence on the situation this task can be the subject of additional constraints like fixed geometry of the network or fixed type of interactions between constituting elements of the network. The importance of the topic has been underlined by the continuous interest it has attracted over the last years [1, 5, 6, 7, 8, 9, 10, 11, 12, 13, 14, 15].

The formal theoretical setting that we employ is deliberately general enough to describe most of the relevant physical systems. These include mainly the systems that have already been used to realize the first QST experiments. We are going to focus on working with the Heisenberg XY Hamiltonians [1].

They naturally describe the spin-spin interactions which are at the core of Nuclear Magnetic Resonance (*NMR*). NMR has been the first method used to demonstrate QST [16, 17, 18, 19]. Another family of physical systems that can be mapped to XY Hamiltonians and that has been demonstrated experimentally capable of QST are the photonic lattices. These are arrays of optical waveguides evanescently coupled together [20]. Over the last years many other systems have been suggested as suitable experimental devices for QST, these include linear arrays of tunnel-coupled dots [3, 21], flying electrons in metals [22], trapped ions [23] and optical lattices [24]. For details on how to map these onto the XY Hamiltonians see [25]. For all the listed systems quality of the transfer is an issue that has to be critically analyzed.

The text is organized as follows. In the first two chapters we give an overview of the theoretical setting of QST. This is where we explore the history of QST which is in an interesting way related to that of angular momentum operators and give several examples of protocols that achieve QST. These include the most famous ones that work with nearest neighbor chains and some beyond-nearest neighbor networks as well, which we initially describe with graph theory. The third chapter is an overview of the Dynamical Decoupling method. Dynamical decoupling is well known to the NMR community [26, 27, 28], it was originally suggested for QIP by Viola et al. [29]. In the fourth chapter we describe the QST on quantum networks using orthogonal polynomials. We present here most of the known properties of QST chains and the state-of-the-art QST next-to-nearest-neighbor protocols. Based on these previously known results we begin to give our own original results.

The first result is the analysis of the joined linear chains presented the in chapter 4.1.2. The second result pertains to quantum state transfer on a rectangular lattice in chapter 4.2.1 and the largest portion of the results relates mainly to imperfect quantum

networks. All physical systems suffer from imperfections, which cannot be ignored in the experimental setups, and limit their performance compared to the ideal case. Quantum networks are certainly no exception. We propose quite a general correction method based on Dynamical Decoupling for several realistic perturbations of some of the known QST protocols. We demonstrate that the method enables improvement of all aspects of QST [7, 30]. These results are reported at length in chapter 5.

Chapter 2

Introduction

2.1 Formalism

Throughout this dissertation we focus on finite quantum networks consisting of $(N+1)$ identical qubits. Specifically we study systems described by the Hilbert space

$$\mathscr{H} = \left(\mathbb{C}^2\right)^{\otimes(N+1)}, \tag{2.1}$$

with the dynamics on it given by the XY Hamiltonians [1, 3, 16, 17, 18, 19, 20, 21, 22, 23, 24]

$$H = \frac{1}{2}\sum_{i=0}^{N}\sum_{j=0}^{N} I_{i,j}\left(\sigma_i^x\sigma_j^x + \sigma_i^y\sigma_j^y\right) + \frac{1}{2}\sum_{i=0}^{N} B_i\left(\sigma_i^z + 1\right). \tag{2.2}$$

Even though this is a rather specific choice, it describes many real physical systems and is quite general. Out of all the physical systems it describes, we choose to use the terminology referring to a magnetic spin-spin interaction. The constants $I_{i,j} \in \mathbb{R}^+$ denote interaction strengths between different sites in the network labeled by $i, j \in \{0, \ldots, N\}$. $B_i \in \mathbb{R}_0^+$ is the strength of the magnetic field acting on qubit i, which is related to the eigenenergy of qubit i. Finally, by σ_i^x we will denote a Pauli operator σ_i^x acting on qubit i

$$\sigma_i^x = \underbrace{\mathbb{I}\otimes\ldots\otimes\mathbb{I}}_{i \text{ times}}\otimes\sigma^x\otimes\ldots\otimes\mathbb{I}, \tag{2.3}$$

$$\sigma^x = \begin{pmatrix} 0 & 1 \\ 1 & 0 \end{pmatrix},\ \sigma^y = \begin{pmatrix} 0 & -i \\ i & 0 \end{pmatrix},\ \sigma^z = \begin{pmatrix} 1 & 0 \\ 0 & -1 \end{pmatrix}. \tag{2.4}$$

Special classes of the Hamiltonians (2.2) are those which impose additional limitations on $I_{i,j}$. For example if

$$I_{i,j} = 0, \text{ for } |i-j| > 1, \tag{2.5}$$

the Hamiltonian describes the *nearest-neighbor* (NN) chain. Or

$$I_{i,j} = 0, \text{ for } |i-j| > 2, \tag{2.6}$$

gives the *next-to-nearest-neighbor* (NNN) chain.

We will use the following definition of Quantum State Transfer (QST) [1]. Consider the system being in the state

$$|\psi_s\rangle = |\psi\rangle |0\rangle \dots |0\rangle , \tag{2.7}$$

where $|0\rangle, |1\rangle$ are the ground and excited states of a qubit and $|\psi\rangle$ is some unknown arbitrary qubit state. If there is a time $T > 0$ such that with probability equal to 1 the system will be in the state

$$|\psi_t\rangle = |0\rangle \dots |0\rangle |\psi\rangle \tag{2.8}$$

we will call that QST from position 0 to N. Without loss of generality we have labeled the starting qubit with the index 0 and the target qubit with N. Naturally there are configurations that do not lead to QST and even the systems that do, will not work for all times. To quantify how close the system is to QST for some process which causes the system to evolve into $|\psi(t)\rangle$, let us define the *fidelity* of state transfer by

$$F(t) = |\langle \psi(t) | \psi_t \rangle| . \tag{2.9}$$

A system allows QST if and only if there is $T > 0$ such that $F(T) = 1$. Since the class of Hamiltonians (2.2) preserves the total number of excitations [1], without loss of generality we can focus on transferring a single excitation in order to achieve QST of an arbitrary state [9]. To see this, we need to use the fact that the Hamiltonian (2.2) commutes with the operator of the number of excitations

$$\left[H, \sum_{i=0}^{N} \sigma_i^z \right] = 0. \tag{2.10}$$

Hence the action of H can be divided into subspaces each corresponding to a fixed number of qubits in an excited state. This means that $|0\rangle \dots |0\rangle$ is an eigenstate of the Hamiltonian and therefore after time T it evolves to

$$|0\rangle \dots |0\rangle \longrightarrow e^{i\varphi} |0\rangle \dots |0\rangle , \tag{2.11}$$

for some $\varphi \in \mathbb{R}$. Let us assume that we have found a system that allows a transfer of a single excitation after time T, therefore we know that the state $|1\rangle |0\rangle \dots |0\rangle$ evolves after time T to

$$|1\rangle |0\rangle \dots |0\rangle \longrightarrow e^{i\eta} |0\rangle |0\rangle \dots |1\rangle , \tag{2.12}$$

for some $\eta \in \mathbb{R}$. We now see that such a system can be easily modified to transfer a general state $\alpha\,|0\rangle + \beta\,|1\rangle\,,\ \alpha, \beta \in \mathbb{C}$, since it evolves after time T to

$$\alpha\,|0\rangle + \beta\,|1\rangle \longrightarrow \alpha e^{i\varphi}\,|0\rangle + \beta e^{i\eta}\,|1\rangle = e^{i\varphi}\left(\alpha\,|0\rangle + \beta e^{i(\eta-\varphi)}\,|1\rangle\right). \tag{2.13}$$

Which can now be corrected to $\alpha\,|0\rangle + \beta\,|1\rangle$ up to a global phase by a simple unitary rotation given by the known φ and η. We therefore focus on finding systems that lead to QST on the single excitation subspace.

Since there is a direct relationship of the systems governed by the XY Hamiltonians and the quantum systems described by the second quantization in the tight-binding approximation [25], the transfer of a single excitation sometimes describes a transfer of an actual particle (bosonic, fermionic systems). Additionally, the transferred particle can have internal degrees of freedom, which can represent the state to be transferred. In such cases only the transfer of a single excitation is considered rather than that of an arbitrary state $|\psi\rangle$.

The input state, the final state and fidelity in the case of single excitation transfer become

$$\begin{aligned} |\psi_s\rangle &= |1\rangle\,|0\rangle \ldots |\ldots\rangle\,, \\ |\psi_t\rangle &= |0\rangle \ldots |0\rangle\,|1\rangle\,, \\ F(t) &= |\langle\psi(t)|0\rangle \ldots |0\rangle\,|1\rangle|\,. \end{aligned} \tag{2.14}$$

It is worth noting that sometimes $F(T)^2$ is used instead to quantify QST since it then becomes the probability of state transfer and, really, it is a matter of preference. We prefer $F(T)$ since if there is time $\hat{T}$ such that we are able the express $\left|\psi(\hat{T})\right\rangle$ as

$$\left|\psi(\hat{T})\right\rangle = a\,|0\rangle \ldots |0\rangle + b\,|0\rangle \ldots |0\rangle\,|1\rangle\,, \tag{2.15}$$

where $a, b \in \mathbb{C}$ are some known coefficients, then in the case of single excitation transfer, $|b|$ *is* the fidelity of QST $F(\hat{T}) = |b|$.

Let us note that the fidelity in the case of single excitation transfer and in the case of the general state $|\psi\rangle$ always allows for a phase change in the desired final state $|\psi_t\rangle$ to $e^{i\varphi}\,|\psi\rangle$. The meaning of this phase is very different in the two cases though. For QST of the general state this is a global phase which, in this case, is irrelevant. In a sharp contrast, if we are considering QST of a single excitation, this phase becomes a relative phase as in Eq. (2.13). If we consider the XY Hamiltonian to describe for example a bosonic system, it is the relative phase between the vacuum state and the single particle state and needs to be corrected for [25].

It is very common to visualize QST processes by plotting the fidelity in time [7], often we are going to consider systems that only achieve QST very probably. In such cases the fidelity never reaches the value one, rather it approaches it arbitrarily close in the fortunate case. It is when the input state only evolves to (2.15) such that $|b| \leq 1$. The reference [13] calls this a *pretty good transfer*. The fidelity in such a case becomes $F(t) \leq 1$. To distinguish between $F(T) < 1$ and $F(T) = 1$, we will sometimes call the latter the *perfect* QST.

If there is a time for which the fidelity reaches 0.95 ($|b| = 0.95$), QST will happen with the probability of 90.25%. This is considered to be the threshold we are going to aim for when correcting for some errors in the networks as its lower bound. In general we are going to work with procedures which can be improved to achieve values arbitrarily close to 1, but in real situation we have to balance between two constraints, the quality of transfer and the effort needed to get there. In order to make the methods comparable, we need to set a standard in order to discuss how *difficult* it is to achieve similar results with different methods.

Since we are mostly going to focus on the single excitation subspace and transfer of an excited state, it will be beneficial to label the vectors that form the *computational basis* as

$$|i\rangle = \underbrace{\underbrace{|0\rangle \ldots |0\rangle}_{i \text{ times}} |1\rangle |0\rangle \ldots |0\rangle}_{(N+1) \text{ vectors}}, \text{ for } i = 0, \ldots N. \tag{2.16}$$

2.1.1 Angular Momentum Analogy

Imperfect QST was first described in 2003 by Bose [2] on an unmodulated spin chain and then a perfect QST was first described independently by Nikolopoulos et al. [3] for electron wavepacket dynamics in the setting of quantum dots and by Christandl et al. [4] in spin networks.

Surprisingly, the dynamics inducing the protocol described in both [3, 4] have already been described in 1979 (when QIP was not fashionable) in a different context [31] of spin systems in homogeneous magnetic fields and of $(N+1)$ level atoms. Since the description of a spin in magnetic fields is widely known, this analogy gives a different view of the QST.

To see this analogy let us identify the states (2.16) from the computational basis $|j\rangle$ with eigenvectors of a J-spin system. One of the common descriptions [32] of a J-spin system uses the eigenvectors of S^2 and one of the components S_z of the spin (angular momentum) operator S labeled by $|m\rangle$, $m \in \{-J, -J+1, \ldots, J\}$. Using these the

correspondence can be defined as

$$\begin{aligned} J &= \frac{N}{2}, \qquad (2.17) \\ N &= 2J, \\ m &= j - \frac{1}{2}N, \qquad (2.18) \\ j &= m + \frac{1}{2}N. \end{aligned}$$

In this form our starting state with $j = 0$ corresponds to $m = -\frac{N}{2}$ and the desired target state with $j = N$ to $m = \frac{N}{2}$.

If we choose

$$B_j = 0, \qquad (2.19)$$

$$\begin{aligned} I_{i,j} &= \frac{\lambda}{2}\sqrt{j(N-j+1)}, \text{ for } j = i+1, \qquad (2.20) \\ I_{i,j} &= 0 \text{ otherwise}, \end{aligned}$$

for $\lambda \in \mathbb{R}^+$ in (2.2), we get a tridiagonal matrix that describes our XY Hamiltonian, and in addition has exactly the same form as a J-spin Hamiltonian in a magnetic field as well as a special case of $N+1$ level atom with Rabi frequency $\Omega_0 = \frac{\lambda}{2}$ [31]. We will call this choice the *Krawtchouk chain* inspired by [10].

The J-spin Hamiltonian of this form describes a spin system in a homogeneous magnetic field in arbitrary direction in the xy plane [31]. It is a known fact [32] that the direction of the spin magnetic moment of a particle in a stationary, homogeneous magnetic field revolves about the axis in the direction of the magnetic field.

It is possible to set up a beautiful representation of the spin (angular momentum) state if it has a well defined value of the projection to z axis (m). In such a state there is still uncertainty in the x and y directions because S_x and S_y do not commute (Heisenberg uncertainty relations). As a result we can represent such a state with a cone in 3D space that has apex in the origin and the base represents the state parameters. Let us place the base along the z axis so that its z coordinate represents m and let us make the radius of it proportional to the uncertainty in x and y. As a result the cones radius is given by

$$r = \sqrt{J(J+1) - m^2}. \qquad (2.21)$$

We will now show how the input and target states are represented in this picture. Since the state $|0\rangle$ corresponds to $m = -\frac{N}{2}$, this state would be plotted as a cone with

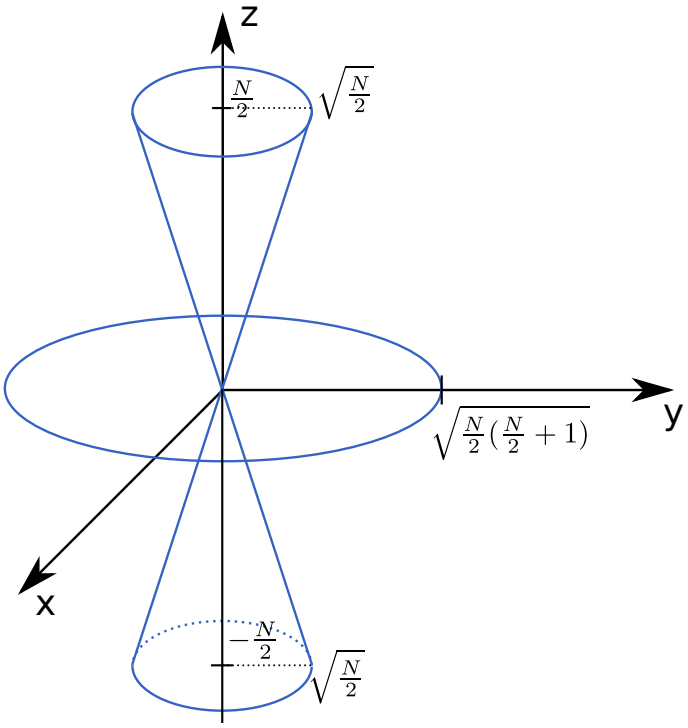

Figure 2.1: Cone representation of the starting, intermediate and target states in the spin representation.

base at $z = -\frac{N}{2}$ and radius $\sqrt{\frac{N}{2}}$. The target state would have the cone base of the same radius, but it would be placed at $z = \frac{N}{2}$. A special case would be $m = 0$ with the excitation present exactly in the middle of the chain, admissible only for odd numbers of qubits $(N + 1)$ (even N), this state would be represented by a disc in the xy plane with radius $\sqrt{\frac{N}{2}(\frac{N}{2}+1)}$.

Since we know that the direction in which the projection of the spin is constant revolves about the axis in the direction the magnetic field, which in this case lies in the xy plane, we already know how the state with $m = -\frac{N}{2}$ is going to evolve. In the cone representation it will expand its base and move it from $z = -\frac{N}{2}$ towards $z = 0$, then all the way to $z = m = \frac{N}{2}$ while narrowing back to the original radius. And then back and forth until infinity. This process is plotted in Fig. 2.1

So just by using the powerful results about the spin systems in magnetic fields and some clever correspondence we have presented a first example of QST. This is probably the most famous one which has been described in many other ways, some of which will be presented in the following subsections. If one writes down the equations of the time

evolution as done in [3, 31], one arrives to a set of partial differential equations. These can be solved with an integral transformation such as the Laplace transform. This can be done by hand and from that one can calculate the time it takes for the state to transform from $m = -\frac{N}{2}$ to $m = \frac{N}{2}$ to be [3, 4]

$$T = \frac{\pi}{\lambda}. \tag{2.22}$$

This approach although very illustrative is not very general, for other choices than those given by Eqs. (2.19), (2.20) the correspondence with angular moment does not work, the Hamiltonian is just too different. Alternative approaches will allow us to uncover additional classes of Hamiltonians (2.2) that lead to QST.

2.1.2 Generating Permutations

Special case of the transformation (2.8) that we defined as QST are all the permutations, which expressed in the computational basis (2.16) have the form of

$$P = \begin{pmatrix} 0 & & & \\ \vdots & & \tilde{P} & \\ 0 & & & \\ 1 & 0 & \dots & 0 \end{pmatrix}, \tag{2.23}$$

where $\tilde{P}$ is an arbitrary permutation matrix.

Košťák et al. gave a method of reconstructing Hamiltonians that lead to such time evolutions in [9]. It is another method of finding QST systems. Let us note right away that the general definition of (2.8) allows for more general $\tilde{P}$, but the first column and the last row are fixed even if $\tilde{P}$ is only some unitary matrix. Without the restriction to permutations the method from [9] becomes difficult to employ since it relies on the known spectra of permutations. As such it might be applicable to other families of unitary transformations with known spectra, but applied to permutations it already provides infinitely many solutions never described before with other methods. It proved being particularly useful and intuitive when the knowledge of the behavior of different subsets of qubits in the chain is needed, such as quantum networks of logical bus topology [33].

We will now rely on the theory of reconstructing self adjoint matrices from their spectra to find QST Hamiltonians. At first we are going to further restrict ourselves

only to one-cycle permutations, namely a very specific permutation

$$P = \begin{pmatrix} 0 & 1 & \dots & 0 \\ \vdots & \ddots & \ddots & \vdots \\ 0 & & 0 & 1 \\ 1 & 0 & \dots & 0 \end{pmatrix}. \tag{2.24}$$

In reality this is not a severe restriction as far as one-cycle permutations go, there are $(N-1)!$ possible one-cycle permutations of the form (2.23) and all of them can be derived from (2.24) just by relabeling the intermediate sites between 0 and N.

Let σ be the spectrum of P, since the characteristic equation for the eigenvalues of the unitary matrix is

$$\lambda^{N+1} = 1, \tag{2.25}$$

we know that the spectrum consists of $N+1$ different complex numbers

$$\lambda_j = \exp\left(2\pi i \frac{j}{N+1}\right), \text{ for } j \in \mathbb{Z}_{N+1}, \tag{2.26}$$

where $\mathbb{Z}_{N+1} = \{0, 1, \dots, N\}$ and i is the imaginary unit.

Straightforward calculation gives the expansion of the corresponding eigenvectors $\left|y_{\lambda_j}\right\rangle$ into the computational basis (2.16):

$$\left|y_{\lambda_j}\right\rangle = \frac{1}{\sqrt{N+1}} \sum_{\alpha=0}^{N} \lambda_j^\alpha \left|\alpha\right\rangle = \frac{1}{\sqrt{N+1}} \begin{pmatrix} 1 \\ \lambda_j^1 \\ \vdots \\ \lambda_j^N \end{pmatrix}. \tag{2.27}$$

The permutation matrix P is diagonal in the basis formed by its eigenvectors, thus

$$P = \sum_{\lambda_j \in \sigma} \lambda_j \left|y_{\lambda_j}\right\rangle \left\langle y_{\lambda_j}\right|. \tag{2.28}$$

The idea is to look for self-adjoint matrices which generate P through the time evolution

$$U(t) = \exp(-iHt), \tag{2.29}$$

for some fixed time $t = T$. Immediately one such solution is

$$H = \frac{-1}{T} \sum_{j=0}^{N} \frac{2\pi j}{N+1} \left|y_{\lambda_j}\right\rangle \left\langle y_{\lambda_j}\right|, \tag{2.30}$$

since this Hamiltonian is diagonal in the basis formed from the eigenvectors of P and thus the exponential (2.29) gives exactly the eigenvalues (2.26) on the diagonal for $t = T$.

Because of the period of the complex exponential in (2.26), we can shift each of the eigenvalues of the Hamiltonian (2.30) by an arbitrary multiple of 2π and we would arrive to the same spectral decomposition of the permutation P and thus to the same permutation. This allows us to expand the solution (2.30) to

$$H_{\vec{l}} = \frac{-1}{T} \sum_{j=0}^{N} \left(\frac{2\pi j}{N+1} + 2\pi l_j \right) |y_{\lambda_j}\rangle \langle y_{\lambda_j}| , \tag{2.31}$$

which is parametrized by a vector of integers $\vec{l} = (l_0, \ldots, l_N) \in \mathbb{Z}^{N+1}$. Since these are all the solutions to the equation (2.25), these are all the Hamiltonians that are the generators of P.

Let us now focus on the connection to the class of Hamiltonians (2.2). To see it, we need to find the values of the coupling constants $I_{i,j}$ and magnetic field strengths B_i in (2.31). Denote by ε_j the

$$\varepsilon_j = -\left(\frac{2\pi j}{N+1} + 2\pi l_j \right) , \tag{2.32}$$

and use the expansion (2.27) to rewrite (2.31) into the computational basis to get:

$$H_{\vec{l}} = \sum_{\alpha,\beta=0}^{N} \sum_{j=0}^{N} \varepsilon_j \lambda_j^{\alpha} \underbrace{\overline{\lambda_j^{\beta}}}_{\lambda_j^{-\beta}} |\alpha\rangle \langle\beta| , \tag{2.33}$$

which for the diagonal terms $\alpha = \beta$ gives

$$B_\alpha = \sum_{j=0}^{N} \varepsilon_j , \tag{2.34}$$

and for the off-diagonal terms

$$I_{\alpha,\beta} = \sum_{j=0}^{N} \varepsilon_j \lambda_j^{\alpha-\beta} . \tag{2.35}$$

To see this, we need to write the Hamiltonian (2.2) in the computational basis:

$$H = \begin{pmatrix} B_0 & I_{0,1} & I_{0,2} & \ldots & I_{0,N} \\ I_{0,1} & B_1 & I_{1,2} & \ldots & I_{1,N} \\ I_{0,2} & I_{1,2} & B_2 & \ldots & I_{2,N} \\ \vdots & \vdots & \vdots & \ddots & \vdots \\ I_{0,N} & I_{1,N} & I_{2,N} & \ldots & B_N \end{pmatrix} . \tag{2.36}$$

These equations mean that any Hamiltonian leading to the permutation P must have identical magnetic fields acting on all its qubits. As mentioned earlier, the most common Hamiltonians for QST assume only nearest neighbor interaction on the qubit chains. In later chapters we are going to show several examples of systems that break this assumption. It is interesting to note here, however, that any Hamiltonian expressed as (2.31) cannot be a nearest neighbor Hamiltonian.

In order to be a nearest neighbor type Hamiltonian, by definition, the following condition must be true

$$I_{\alpha,\beta} = 0 \text{ for } \alpha - \beta \neq \pm 1. \tag{2.37}$$

Since we know that $I_{\alpha,\beta}$ are given by Eq. (2.35), this gives $N-1$ equations for ε_j, in matrix form given as

$$\begin{pmatrix} \lambda_0^2 & \lambda_1^2 & \dots & \lambda_N^2 \\ \lambda_0^3 & \lambda_1^3 & \dots & \lambda_N^3 \\ \vdots & & & \vdots \\ \lambda_0^N & \lambda_1^N & \dots & \lambda_N^N \end{pmatrix} \begin{pmatrix} \varepsilon_0 \\ \vdots \\ \varepsilon_N \end{pmatrix} = \begin{pmatrix} 0 \\ \vdots \\ 0 \end{pmatrix}. \tag{2.38}$$

This is a matrix equation of the discrete Fourier transform with the first two rows and normalization $1/\sqrt{N+1}$ dropped (see Eq. (2.26)). Therefore the solutions are known and since we are looking for real solutions (eigenvalues of a self-adjoint matrix), they are limited to

$$\begin{pmatrix} \varepsilon_0 \\ \vdots \\ \varepsilon_N \end{pmatrix} = \gamma \begin{pmatrix} 1 \\ \vdots \\ 1 \end{pmatrix}, \tag{2.39}$$

for some $\gamma \in \mathbb{R}$. However such a solution gives also $I_{\alpha,\beta} = 0$ for all α and β from how a constant vector is transformed through discrete Fourier transform. We have thus shown that if the Hamiltonian is nearest neighbor, not even the nearest neighbors are allowed to interact. There is no such Hamiltonian (2.33) that would lead to QST.

Many-cycle Permutations

Until now we have only focused on one-cycle permutations. If the permutation is a many cycle permutation, i.e. it can be expressed as a product of n cycles

$$P = P^{(0)} \dots P^{(n)}, \tag{2.40}$$

it turns out that finding the respective generating Hamiltonians only involves applying the one cycle procedure to every cycle of the permutation. Let us fix on some specific

cycle $P^{(i)}$ first. By $S_d \subset \mathbb{Z}_{N+1}$ we denote the subset of $d+1$ qubits that it affects. Similarly to (2.26) it has the eigenvalues given by

$$\lambda_j = \exp\left(2\pi i \frac{j}{d+1}\right),\ j \in \mathbb{Z}_{d+1}. \tag{2.41}$$

Now the spectrum σ of P is a union of the individual spectra for each cycle and we can immediately see that as long as the permutation has at least two cycles ($n \geq 2$), the spectrum is always going to be degenerate. Let us denote by δ_j the degeneracy of the eigenvalue λ_j. δ_j is the number of different cycles that have the same eigenvalue, therefore for every $k \in \{0, \ldots, \delta_j - 1\}$ the corresponding eigenvectors $\left|v_{\lambda_j}^{(k)}\right\rangle$ can be expanded similarly to (2.27) as

$$\left|v_{\lambda_j}^{(k)}\right\rangle = \sum_{\alpha \in S_d^{(k)}} \frac{\lambda_j^\alpha}{\sqrt{d+1}} \left|\alpha\right\rangle, \tag{2.42}$$

where $S_d^{(k)}$ is the corresponding subset of qubits involved in the cycle that contributed the k-th eigenvalue λ_j to σ.

In exactly the same manner as we arrived to the expression (2.31), we can now shift the phase of every λ_j, but we can do it δ_j times for each eigenvalue. Essentially, we have more freedom in choosing the Hamiltonians that generate the permutation (2.40). Another freedom is in the choice of the basis of each eigen subspace, we can move from $\left|v_{\lambda_j}^{(k)}\right\rangle$ to some other basis which we will denote by $\left|y_{\lambda_j}^{(k)}\right\rangle$. Putting this together we can express all the Hamiltonians that lead to a given many cycle permutation as

$$H_{\vec{l}} = \frac{-1}{T} \sum_{\lambda_j \in \sigma} \sum_{k=0}^{\delta_j - 1} \left(\arg(\lambda_j) + 2\pi l_j^{(k)}\right) \left|y_{\lambda_j}^{(k)}\right\rangle \left\langle y_{\lambda_j}^{(k)}\right|, \tag{2.43}$$

where $\vec{l} \in \mathbb{Z}^{N+1}$.

Many Cycle Example

So far we have focused on the first column and last row in the form of the time evolution (2.23) since that is how we defined QST. However, it is known [1], and from the analogy with the angular momentum operators in chapter 2.1.1 it can be seen, that the choice of couplings (2.20) in the Hamiltonian (2.2) leads to a unitary evolution that acts on the remainder of the qubits as the many-cycle permutation

$$P = \begin{pmatrix} 0 & & 1 \\ & \iddots & \\ 1 & & 0 \end{pmatrix}. \tag{2.44}$$

We would now like to show how it is possible to come to the couplings (2.20) in the framework of many cycle permutations.

We will focus on the example presented in [9] of a four qubit system and the permutation

$$P = \begin{pmatrix} 0 & 0 & 0 & 1 \\ 0 & 0 & 1 & 0 \\ 0 & 1 & 0 & 0 \\ 1 & 0 & 0 & 0 \end{pmatrix}, \tag{2.45}$$

and see on it how the procedure would work for higher numbers of qubits.

Now P is a two cycle permutation

$$P = P^{(0)}P^{(1)} = \begin{pmatrix} 0 & 0 & 0 & 1 \\ 0 & 1 & 0 & 0 \\ 0 & 0 & 1 & 0 \\ 1 & 0 & 0 & 0 \end{pmatrix} \begin{pmatrix} 1 & 0 & 0 & 0 \\ 0 & 0 & 1 & 0 \\ 0 & 1 & 0 & 0 \\ 0 & 0 & 0 & 1 \end{pmatrix}, \tag{2.46}$$

and both the cycles have two eigenvalues $\lambda_0 = e^{i0} = 1$ and $\lambda_1 = e^{i\pi} = -1$. So the permutation P has the same eigenvalues, which are doubly degenerate.

The eigenvectors (2.42) corresponding to the eigenvalues ± 1 expressed in the computational basis (2.16) are

$$\begin{aligned} \left|v_{\pm}^{(0)}\right\rangle &= \frac{1}{\sqrt{2}}\left(|0\rangle \pm |3\rangle\right), \\ \left|v_{\pm}^{(1)}\right\rangle &= \frac{1}{\sqrt{2}}\left(|1\rangle \pm |2\rangle\right). \end{aligned} \tag{2.47}$$

One of the freedoms for many cycle permutations is choosing the eigen basis, let us introduce a new basis from the original eigenvectors with four complex numbers $\mu, \nu, \zeta, \xi \in \mathbb{C}$ as

$$\begin{aligned} \left|y_{+}^{(0)}\right\rangle &= \nu\left|v_{+}^{(0)}\right\rangle + \mu\left|v_{+}^{(1)}\right\rangle, \\ \left|y_{+}^{(1)}\right\rangle &= \overline{\mu}\left|v_{+}^{(0)}\right\rangle - \overline{\nu}\left|v_{+}^{(1)}\right\rangle, \\ \left|y_{-}^{(0)}\right\rangle &= \xi\left|v_{-}^{(0)}\right\rangle + \zeta\left|v_{-}^{(1)}\right\rangle, \\ \left|y_{-}^{(1)}\right\rangle &= \overline{\zeta}\left|v_{-}^{(0)}\right\rangle - \overline{\xi}\left|v_{-}^{(1)}\right\rangle, \end{aligned} \tag{2.48}$$

$$\tag{2.49}$$

where $|\mu|^2 + |\nu|^2 = 1$ and $|\zeta|^2 + |\xi|^2 = 1$.

In this basis, if we take advantage of the freedom in shifting phases of each eigenvalue, we can write down all the Hamiltonians that generate the permutation P from (2.43):

$$\begin{aligned} H_{\vec{l}} = \frac{-1}{T} \Big(& (0 + 2\pi l_+^{(0)}) \left| y_+^{(0)} \right\rangle \left\langle y_+^{(0)} \right| + \\ & (0 + 2\pi l_+^{(1)}) \left| y_+^{(1)} \right\rangle \left\langle y_+^{(1)} \right| + \\ & (\pi + 2\pi l_-^{(0)}) \left| y_-^{(0)} \right\rangle \left\langle y_-^{(0)} \right| + \\ & (\pi + 2\pi l_-^{(1)}) \left| y_-^{(1)} \right\rangle \left\langle y_-^{(1)} \right| \Big), \end{aligned} \tag{2.50}$$

which can be relabeled to

$$\begin{aligned} H_{\vec{l}} = & \varepsilon_+^{(0)} \left| y_+^{(0)} \right\rangle \left\langle y_+^{(0)} \right| + \\ & \varepsilon_+^{(1)} \left| y_+^{(1)} \right\rangle \left\langle y_+^{(1)} \right| + \\ & \varepsilon_-^{(0)} \left| y_-^{(0)} \right\rangle \left\langle y_-^{(0)} \right| + \\ & \varepsilon_-^{(1)} \left| y_-^{(1)} \right\rangle \left\langle y_-^{(1)} \right|. \end{aligned} \tag{2.51}$$

Furthermore because of the form of the eigenvectors, all the Hamiltonians (2.51) have to be persymmetric (symmetric along the antidiagonal), we will later see that this is a necessary condition for any QST Hamiltonian, not just the ones connected to permutations.

Without additional constraints we can generate infinitely many Hamiltonians by simply choosing different integer vectors $\vec{l}$ and the complex numbers μ, ν, ζ, ξ. However, we would like to find among these all the NN Hamiltonians:

$$H_{\vec{l}} = \begin{pmatrix} E_0 & g_1 & 0 & 0 \\ g_1 & E_1 & g_2 & 0 \\ 0 & g_2 & E_1 & g_1 \\ 0 & 0 & g_1 & E_0 \end{pmatrix}. \tag{2.52}$$

Expanding (2.51) in the computational basis now gives 16 equations for $\vec{l}$ and μ, ν, ζ, ξ. It can be shown by hand that this system does not have a solution for Hamiltonians with a degenerate spectrum. Therefore let us assume that the Hamiltonian has a non-degenerate spectrum.

The first equations we are going to write out are for the elements $\langle 0| H_{\vec{l}} |2\rangle$ and $\langle 1| H_{\vec{l}} |3\rangle$. These are respectively:

$$\varepsilon_+^{(0)} |\nu|^2 + \varepsilon_+^{(1)} |\mu|^2 - \varepsilon_-^{(0)} |\xi|^2 - \varepsilon_-^{(1)} |\zeta|^2 = 0, \tag{2.53}$$

$$(\varepsilon_+^{(0)} - \varepsilon_+^{(1)}) \nu \overline{\mu} + (\varepsilon_-^{(1)} - \varepsilon_-^{(0)}) \xi \overline{\zeta} = 0 \tag{2.54}$$

The general Hamiltonian is symmetric in ways that these two guarantee all the required zeroes in the Hamiltonian (2.52). Since we required μ, ν and ζ, ξ to be normalized, the equation for $\langle 0| H_{\vec{l}} |2\rangle$ can be written as

$$(\varepsilon_+^{(0)} - \varepsilon_+^{(1)}) |\nu|^2 - (\varepsilon_-^{(0)} - \varepsilon_-^{(1)}) |\xi|^2 + \varepsilon_+^{(1)} - \varepsilon_-^{(1)} = 0. \tag{2.55}$$

And this is the first time that we found the QST property of a Hamiltonian to depend on the differences of the eigenvalues of the Hamiltonian. In later sections we are going to show that a very specific condition on the differences of eigenvalues is actually equivalent to the Hamiltonian having the QST property. So note that if $\varepsilon_0, \varepsilon_1, \varepsilon_2, \varepsilon_3$ are a solution to the system of equations, so is $\{\varepsilon_0 + 2\pi j, \varepsilon_1 + 2\pi j, \varepsilon_2 + 2\pi j, \varepsilon_3 + 2\pi j\}$ for some $j \in \mathbb{Z}$.

The two equations from $\langle 0| H_{\vec{l}} |2\rangle$ and $\langle 1| H_{\vec{l}} |3\rangle$ essentially fix the parameters μ, ν, ζ, ξ up to their phase, the solutions are

$$\begin{aligned}
|\mu| &= \sqrt{\frac{(\varepsilon_+^{(1)} - \varepsilon_-^{(1)})(\varepsilon_-^{(0)} - \varepsilon_+^{(1)})}{(\varepsilon_+^{(0)} - \varepsilon_+^{(1)})(\varepsilon_+^{(0)} - \varepsilon_-^{(1)} - \varepsilon_-^{(0)} + \varepsilon + -^{(1)})}}, \\
|\nu| &= \sqrt{\frac{(\varepsilon_-^{(0)} - \varepsilon_+^{(0)})(\varepsilon_-^{(1)} - \varepsilon_+^{(0)})}{(\varepsilon_+^{(0)} - \varepsilon_+^{(1)})(\varepsilon_+^{(0)} - \varepsilon_-^{(1)} - \varepsilon_-^{(0)} + \varepsilon + -^{(1)})}}, \\
|\xi| &= \sqrt{\frac{(\varepsilon_-^{(1)} - \varepsilon_+^{(0)})(\varepsilon_-^{(1)} - \varepsilon_+^{(1)})}{(\varepsilon_-^{(0)} - \varepsilon_-^{(1)})(\varepsilon_+^{(0)} - \varepsilon_-^{(1)} - \varepsilon_-^{(0)} + \varepsilon + -^{(1)})}}, \\
|\zeta| &= \sqrt{\frac{(\varepsilon_-^{(0)} - \varepsilon_+^{(0)})(\varepsilon_-^{(0)} - \varepsilon_+^{(1)})}{(\varepsilon_-^{(1)} - \varepsilon_-^{(0)})(\varepsilon_+^{(0)} - \varepsilon_-^{(1)} - \varepsilon_-^{(0)} + \varepsilon + -^{(1)})}},
\end{aligned} \tag{2.56}$$

with the additional condition on φ and χ, which are defined as $\mu = e^{i\varphi} |\mu|$ and $\zeta = e^{i\chi} |\zeta|$:

$$\varphi - \chi = m\pi, \ m \in \mathbb{Z}, \tag{2.57}$$

and m being odd for

$$\frac{\varepsilon_+^{(0)} - \varepsilon_+^{(1)}}{\varepsilon_-^{(0)} - \varepsilon_-^{(1)}} < 0, \tag{2.58}$$

and even otherwise.

The normalization conditions and the positivity of the arguments of the square roots in (2.56) together imply that the intervals $[\varepsilon_+^{(0)}, \varepsilon_+^{(1)}]$ and $[\varepsilon_-^{(0)}, \varepsilon_-^{(1)}]$ must overlap but are not allowed to contain one another.

The remaining equations for

$$\begin{aligned} \langle 0| H_{\vec{l}} |0\rangle &= E_0, \\ \langle 1| H_{\vec{l}} |1\rangle &= E_1, \\ \langle 0| H_{\vec{l}} |1\rangle &= g_1, \\ \langle 1| H_{\vec{l}} |2\rangle &= g_2, \end{aligned} \tag{2.59}$$

can always be solved for a particular choice of the diagonal and off diagonal elements. Since the spectrum of the J-spin Hamiltonian fulfills all of the above conditions for $J = 3/2$, for any choice of λ and T there exist $\vec{l}$ and μ, ν, ζ, ξ such that the Hamiltonian (2.2) with couplings (2.20) and magnetic fields (2.19) is obtained within this framework.

For example for $\lambda = 2$, $T = \pi/\lambda$, $E_0 = E_1 = B = 3$, $g_1 = I_1 = \frac{\lambda}{2}\sqrt{3}$, $g_2 = I_2 = \frac{\lambda}{2}\sqrt{4}$ taken from (2.20) a solution is

$$\begin{aligned} l_+^{(0)} &= 0, \\ l_+^{(1)} &= -1, \\ l_-^{(0)} &= -1, \\ l_-^{(1)} &= -2, \end{aligned} \tag{2.60}$$

which is exactly the Krawtchouk chain with additional global magnetic field that only adds a global phase to the time evolution.

Higher dimensions have to be addressed separately in this framework, but the outlined approach is applicable rather straightforwardly. Several more examples of QST Hamiltonians that can be obtained with this framework are given in [9].

2.1.3 QST on Graphs

The different topologies of QST systems given by specifying which qubits are interacting with its neighbors are easily expressed with graph theory. Numerous examples of how to exploit the language of graphs in order to construct QST networks can be found in [13]. We are going to give an overview of the formalism and the most simple examples.

Let G be a graph, V the set of its vertices and E the set of its edges. For simplicity we are not going to allow edges to have neither orientation nor length, hence the adjacency matrix (Laplacian) A of G only has one and zero elements. Several generalizations of these simplifications have already been found [34, 15], but for our purposes this is going to be sufficient. This setting is often called a *continuous time quantum walk* [35, 36]. In the later section 4.1.4 we are going to show how to connect the formalism of 2.1 with

the one of graphs by showing that the protocol (2.20) is essentialy a continuous time quantum random walk on a hypercube.

Since the graph is not oriented, the adjacency matrix is real and symmetric. Therefore, if we calculate its exponential

$$U(t) = \exp(-iAt), \tag{2.61}$$

again, we get a symmetric matrix. In the setting of graphs we say that state transfer occurs between sites u and v after time T if

$$|U(T)_{u,v}| = 1, \tag{2.62}$$

where the lower indexes denote the element (u, v) of the respective matrix.

We can now see that the definitions of QST from section 2.1 and this one are the same if we take the adjacency matrix to be the Hamiltonian on the space (2.1) expressed in the computational basis (2.16) in the sense of QST of a single excitation. Even though the definitions are the same, the Hamiltonians given by the simple adjacency matrices are much less general than those from (2.2). Essentially we restrict ourselves to $J_{i,j}$ and B_i being ones and zeroes. Nevertheless we are going to show how to find graphs with the QST property.

Let us start by the simplest example. Consider G to be the graph K_2, which has two elements and its adjacency matrix is

$$A = \begin{pmatrix} 0 & 1 \\ 1 & 0 \end{pmatrix}. \tag{2.63}$$

By a simple calculation

$$U(t) = \cos(t)\mathbb{I} - i\sin(t)A = \begin{pmatrix} \cos(t) & -i\sin(t) \\ -i\sin(t) & \cos(t) \end{pmatrix}. \tag{2.64}$$

For $t = \pi/2$ it gives

$$U\left(\frac{\pi}{2}\right) = \begin{pmatrix} 0 & -i \\ -i & 0 \end{pmatrix}, \tag{2.65}$$

therefore $\left|U\left(\frac{\pi}{2}\right)_{0,1}\right| = |-i| = 1$. Obviously the same is true for $t = T = \frac{\pi}{2} + k\pi$, where $k \in \mathbb{Z}$.

Since $U(t)$ is a symmetric matrix, it is obviously true, that if $|U(T)_{u,v}| = 1$ for some T, it is also true that $|U(t)_{v,u}| = 1$. Therefore if there is QST from u to v, then there is QST from v to u.

Because the condition (2.62) is equivalent to

$$U(T)\left|u\right\rangle = e^{i\varphi}\left|v\right\rangle, \tag{2.66}$$

for some $\varphi \in \mathbb{R}$ and because if the graph transfers state from u to v, it transfers it vice versa as well, the following is also true

$$U(T)^2\left|u\right\rangle = e^{2i\varphi}\left|u\right\rangle. \tag{2.67}$$

So we see that if the system transfers state after time T, the time evolution is periodic with period $2T$ since $\exp(-iAt)^2 = \exp(-2iAt)$.

Combining QST Graphs

In order to show how to generate infinitely many graphs with the QST property, we need to define a Cartesian product of two graphs X and Y denoted by $X \times Y$. Let us define it by a graph with vertices given by the Cartesian product of the vertices of the original graph $V(X \times Y) = V(X) \times V(Y)$ and adjacency matrix given by

$$A(X \times Y) = A(X) \otimes \mathbb{I} + \mathbb{I} \otimes A(Y). \tag{2.68}$$

It is straightforward to define a d-th Cartesian power of a graph X by

$$X^d = \underbrace{X \times \ldots \times X}_{d \text{ times}} \tag{2.69}$$

These definitions are quite opaque at first, but consider for example a path of length m denoted by P_m which for $m = 2$ is just a line segment of length one. Now the second power P_2^2 is just a square and P_2^d is a d-dimensional cube.

Since $A(X \times Y)$ is a sum of two commuting matrices, the following is not difficult to prove

$$U_{A(X\times Y)}(t) = U_{A(X}(t) \otimes U_{A(Y)}(t). \tag{2.70}$$

A corollary of this equation is the fact that if we have a graph X which after time T transfers state from u to v, X^d transfers state between the d-tuples $(u, \ldots, u)$ and $(v, \ldots, v)$ after the same time T. Therefore we have shown that a d-cube transfers state since we know that $P_2 = K_2$ which transfers state from $u = 0$ to $v = 1$ and vice versa.

One might consider going to higher m in the paths P_m. Let us first focus on the case of P_3. Explicit calculation by finding the three eigenvectors of the adjacency matrix

$$A(P_3) = \begin{pmatrix} 0 & 1 & 0 \\ 1 & 0 & 1 \\ 0 & 1 & 0 \end{pmatrix}, \tag{2.71}$$

gives

$$U\left(\frac{\pi}{\sqrt{2}}\right) = \begin{pmatrix} 0 & 0 & -1 \\ 0 & -1 & 0 \\ -1 & 0 & 0 \end{pmatrix}. \tag{2.72}$$

This means that P_3 transfers state between $u = 0$ and $v = 2$ and vice versa. Notice that we already know this since this is a special case of (2.20). Therefore we know that any Cartesian power P_3^d for arbitrary $d \in \mathbb{N}$ transfers state. We have thus found two infinite families of graphs that transfer state. Compared to nearest or even next-to-nearest neighbor chains these networks are however much more connected and for higher d constructing real physical experiments with that many interacting sites might pose an obstacle.

It turns out that going to higher m is not possible. The limiting factors are the unit coupling strengths. The proof of this and many other examples of graphs that lead to QST can be found in [13]. We will show how this formalism can for a special graph choice be translated to non unitary couplings later in the chapter 4.1.4 using orthogonal polynomials.

After laying out the elementary properties of network serving for QST we turn our attention to the performance of such network under realistic conditions and ways how to improve its performance in cases of imperfections.

Chapter 3

Dynamical Decoupling

3.1 Imperfect World

Imagine a situation where you are trying to create a system of several interacting systems, such as qubits, whose dynamics is prescribed by some Hamiltonian H_{id}. Unwanted interactions inevitably occur and all you are left with is some real Hamiltonian H instead, which might or might not be in some way close to the ideal (design) Hamiltonian. In such a situation we desire to recast the whole problem or, when possible, manipulate the real Hamiltonian to come close to the original form. There are several methods how to accomplish such a task and Dynamical decoupling is one of them. Without loss of generality let us assume that both H and H_{id} are traceless. In such a situation Dynamical Decoupling gives a scheme, a sequence of unitary operators, which when applied periodically to your system, causes the system to evolve as it would under H_{id} [29]. We are going to assume the so called *bang-bang* control, a possibility of instantaneous application of the pulses realizing unitary operations of the decoupling.

The bang-bang control lies somewhere between the two extremes of the known correction procedures. One relies on the passive restriction to states that are resistant to the perturbations, which is commonly referred to as *decoherence free subspaces* [37] while the other, *quantum error correcting codes* [38], relies on a feedback loop of control pulses applied based on measurements realized on the system. Similar in spirit to the bang-bang control is the *quantum Zeno mechanism* [39] which instead of periodic application of unitary pulses stabilizes the time evolution of a system by quick repeated measurements which force the system to one of the eigenstates of the measured observable. The fundamental difference between the other correction methods and Dynamical Decoupling is that the time evolution is unitary in the dynamical decoupling case.

The time scales of the control pulses are assumed to be much shorter than the time it will take for the desired time evolution to take place (bang-bang control is an approximation of instantaneous interventions [29]) which is a non trivial requirement that has to be addressed individually for each quantum system. For example in the case of electron and nuclear spin states in the endohedral fullerene molecule NC_{60} the bang bang pulses to the nuclear state can be done due to the spin-spin interaction and much quicker response times to external magnetic fields of the electron compared to the nucleus [28].

The bang-bang control consists of a sequence of m unitary pulses $p_0, \ldots, p_m$. Furthermore, let us restrict ourselves to a situation where the pulses are always applied after the same amount of time Δt and we will allow each pulse to act only as representing one of the $\{\mathbb{I}, \sigma^x, \sigma^y, \sigma^z\}$ operators on each qubit. Therefore we can write the unitary operator of time evolution after time T

$$U(T) = p_m e^{-iH\Delta T} p_{m-1} e^{-iH\Delta T} \ldots p_1 e^{-iH\Delta T} p_0. \tag{3.1}$$

It turns out that for upcoming calculations it is beneficial to rewrite this evolution into a different form. Let us introduce new operators

$$g_k = p_k p_{k-1} \ldots p_0. \tag{3.2}$$

It is very straightforward to notice that this is equivalent to

$$p_k = g_k g_{k-1}^\dagger. \tag{3.3}$$

With these new labels $U(T)$ becomes

$$U(T) = g_m \left(g_{m-1}^\dagger e^{-iH\Delta T} g_{m-1} \right) \ldots \left(g_0^\dagger e^{-iH\Delta T} g_0 \right). \tag{3.4}$$

Since the original operators p_k were unitary, the operators g_k are unitary as well and we can move them into the exponent

$$U(T) = g_m e^{-i\left(g_{m-1}^\dagger H g_{m-1}\right)\Delta T} \ldots e^{-i\left(g_0^\dagger H g_0\right)\Delta T}. \tag{3.5}$$

This time evolution can be expanded with the Magnus expansion [40] to obtain the *average* Hamiltonian $\overline{H}$. This Hamiltonian then generates the same time evolution

$$U(T) = g_m e^{-i\overline{H}T}. \tag{3.6}$$

For simplicity let us further assume that g_m can be chosen to be the identity $g_m = \mathbb{I}$. This means having $p_m = g_{m-1}^\dagger$. If this represents an obstacle, we can always work in a rotated frame induced by the operator g_m.

We can use the Magnus expansion to explicitly calculate the expansion of the average Hamiltonian $\overline{H}$ into increasing powers of ΔT

$$\overline{H} = \overline{H}^{(0)} + \overline{H}^{(1)} + \dots. \tag{3.7}$$

The lowest order approximation is given by

$$\overline{H}^{(0)} = \frac{1}{m} \sum_{k=0}^{m-1} g_k^\dagger H g_k. \tag{3.8}$$

It can be shown [40] that the remaining terms are proportional to the respective powers of ΔT

$$\overline{H}^{(k)} = O\left((m\Delta T)^k\right). \tag{3.9}$$

This means that the shorter the time intervals between successive pulses are, the better the lowest order approximation becomes.

Since we want to use Dynamical Decoupling as a correction method, we can see that in the lowest order we should require that

$$\overline{H}^{(0)} = \frac{1}{m} \sum_{k=0}^{m-1} g_k^\dagger H g_k = \frac{1}{D} H_{\mathrm{id}}, \tag{3.10}$$

where we allowed for some scaling of time $D \in \mathbb{R}^+$. If this equation holds, the system is effectively going to evolve as if its Hamiltonian were H_{id} and not H.

In the equation (3.10) the Hamiltonians are known and we are searching for $\{g_k\}_{k=0}^{m-1}$, a set of unitary operators which allow the design of the desired correction. If we are able to find such operators, we will call them a *selective decoupling scheme* [7].

3.2 Improving Decoupling Schemes

For the moment let us assume that we found a decoupling scheme. In the upcoming sections we show that this is always possible, under very natural assumptions. We are looking for simple ways to improve it, since it is only an approximation. This can be accomplished using several *tricks*.

As mentioned earlier, the shorter ΔT, the better the approximation. If we have a decoupling scheme $\{g_k\}_{k=0}^{m-1}$, we can define for some $l \in \mathbb{N}$ another decoupling scheme of $(l \cdot m)$ operators $\{\tilde{g}_k\}_{k=0}^{lm-1}$ by

$$\tilde{g}_k = g_{k \bmod m}. \tag{3.11}$$

If the original scheme gave operators applied in ΔT intervals, the derived scheme is to be applied in Δ / l intervals.

To see that this is a decoupling scheme as well, just write out the main condition (3.10) and assume it holds for $\{g_k\}_{k=0}^{m-1}$, then

$$\frac{1}{lm}\sum_{k=0}^{lm-1}\tilde{g}_k^\dagger H\tilde{g}_k = \frac{1}{lm}l\sum_{k=0}^{m-1}g_k^\dagger H g_k = \frac{1}{D}H_{\mathrm{id}}. \tag{3.12}$$

This trick is usually called a *periodic decoupling scheme*.

Another trick we are going to employ is the permutation of some decoupling scheme $\{g_k\}_{k=0}^{m-1}$. It stems from the fact that the sum in (3.10) is independent of ordering of the operators in the scheme. So, if one takes some permutation of indexes $\pi(k)$ and creates a sequence $\{g_{\pi k}\}_{k=0}^{m-1}$, one immediately arrives at another decoupling scheme again.

In general there is no optimal permutation to be found, there are however some permutations which should always lead to an improved scheme. One of the often used permutations is the permutation of the periodic decoupling scheme with $l = 2$. For such a scheme we can define the permutation as

$$\pi(k) = \begin{cases} k, & \text{if } k < m. \\ 2m-k-1, & \text{otherwise.} \end{cases} \tag{3.13}$$

We arrive at the so called *symmetric decoupling scheme*. This procedure eliminates all the odd orders in the Magnus expansion [41] thus further improving any decoupling scheme.

Usually the two tricks are employed together. We achieved the best performance in simulations by proceeding in two steps, first we make the schemes symmetric, then periodic.

3.3 Finding Decoupling Schemes

As already mentioned, there are several ways of finding solutions of (3.10). First we are going to present an algorithm which also demonstrates that we can always find a solution under a very natural requirement, which is easy to meet.

In order to simplify the notation, we are going to work with multiindexes. Since the set of four matrices

$$\{s_j\}_{j=0}^{3} \equiv \{\mathbb{I}, \sigma^x, \sigma^y, \sigma^z\}, \tag{3.14}$$

forms a basis of operators acting on $\mathbb{C}^2$, and since

$$\{S_j\}_{j=0}^{4^{(N+1)}-1} \equiv \{s_{j_0}\otimes s_{j_1}\ldots\otimes s_{j_N}\}_{j_0,\ldots,j_N=0}^{4}, \tag{3.15}$$

forms a basis of all operators on $\left(\mathbb{C}^2\right)^{\otimes(N+1)}$, it immediately follows that we can take the index j on the left hand side of (3.15) and turn it into a corresponding multiindex on the right hand side simply by writing it in base four, the digits now give individual indices.

We are now going to expand the Hamiltonians H and H_{id} from (3.10) in this basis and label the coefficients as μ_j and ν_j

$$H = \sum_{j=0}^{4^{(N+1)}-1} \mu_j S_j, \tag{3.16}$$

$$H_{\mathrm{id}} = \sum_{j=0}^{4^{(N+1)}-1} \nu_j S_j. \tag{3.17}$$

Since we assumed the Hamiltonians to be traceless, we already know that

$$\mu_0 = \nu_0 = 0, \tag{3.18}$$

since $S_0 = \mathbb{I}$.

Plugging these expansions into the main decoupling condition (3.10) gives

$$\frac{D}{m} \sum_{j=1}^{4^{(N+1)}-1} \sum_{k=0}^{m-1} g_k^\dagger \mu_j S_j g_k = \sum_{j=1}^{4^{(N+1)}-1} \nu_j S_j. \tag{3.19}$$

Since we restricted ourselves to p_k being one of the basis operators, from the properties of Pauli matrices immediately follows that g_k are one of the basis operators as well up to a phase

$$g_l = e^{i\varphi} S_m, \tag{3.20}$$

for all $l \in \{0 \dots m-1\}$ and some $m \in \{0 \dots 4^{N+1}-1\}$. If we label the number of times that the operator $S_k = S_k^\dagger$ appears in the decoupling scheme $\{g_k\}_{k=0}^{m-1}$ by c_k, this equation becomes

$$\frac{D}{m} \sum_{j=1}^{4^{(N+1)}-1} \sum_{k=0}^{4^{(N+1)}-1} c_k \mu_j S_k S_j S_k = \sum_{j=1}^{4^{(N+1)}-1} \nu_j S_j. \tag{3.21}$$

One of the basic properties of the operators s_j from (3.14) (Pauli operators) is

$$s_j^\dagger s_k^\dagger s_j s_k = \pm s_0. \tag{3.22}$$

Therefore the same holds for

$$S_j^\dagger S_k^\dagger S_j S_k = \pm S_0. \tag{3.23}$$

We can now label the signs by $a_{j,k}$

$$S_j^\dagger S_k^\dagger S_j S_k = a_{j,k} S_0, \tag{3.24}$$

and arrive at

$$\frac{D}{m} \sum_{j=1}^{4^{(N+1)}-1} \sum_{k=0}^{4^{(N+1)}-1} c_k \mu_j a_{j,k} S_j = \sum_{j=1}^{4^{(N+1)}-1} \nu_j S_j. \tag{3.25}$$

Because S_j form a basis, the equation (3.25) gives at most $4^{N+1}-1$ linear equations for 4^{N+1} variables c_k, which is not prohibitive for the existence of solutions.

We are now able to specify exactly under which conditions we can solve the system of equations (3.25). A major restriction appears if for any j the expansion coefficient of the Hamiltonian H is $\mu_j = 0$. In this case we immediately know that $\nu_j = 0$ as well. This is a significant restriction on the class of the problems that Dynamical Decoupling is applicable to. By Dynamical Decoupling one cannot create terms not present in the original Hamiltonian. This is an essential feature of the method and we have to keep it in mind when discussing limitations and applicability of it.

We now show that if $\mu_j = 0$ implies $\nu_j = 0$, the system has infinitely many solutions. To prove this claim, let us write the system of linear equations explicitly.

$$\frac{D}{m} \sum_{k=0}^{4^{N+1}-1} a_{j,k} c_k = \frac{\nu_j}{\mu_j},\ j \in \mathscr{J}, \tag{3.26}$$

$$\mathscr{J} = \left\{ j \in \{1, \ldots, 4^{N+1}-1\} : \mu_j \neq 0 \right\}. \tag{3.27}$$

This is a system of equations for the 4^{N+1} variables c_k, however D and m defined earlier are unknown as well. The last two variables are not independent of c_k though, so we can simplify the equations by introducing new variables

$$e_k \equiv \frac{D c_k}{m}, \tag{3.28}$$

and the system of equations (3.26) becomes

$$\sum_{k=0}^{4^{N+1}-1} a_{j,k} e_k = \frac{\nu_j}{\mu_j},\ j \in \mathscr{J}. \tag{3.29}$$

If we are able to solve (3.29) for e_k, D is immediately found from

$$D = \sum e_k, \tag{3.30}$$

and m should be found as the smallest common denominator of the set of rational numbers

$$\left\{\frac{e_k}{D}\right\}_{k=0}^{4^{N+1}-1}. \tag{3.31}$$

For the system of $N+1$ qubits, the earlier introduced plus and minus ones $a_{j,k}$ can be cast into a matrix

$$A^{(N+1)} = (a_{j,k}). \tag{3.32}$$

For $N = 0$ this matrix can be calculated from the Pauli matrices

$$A^{(1)} = \begin{pmatrix} 1 & 1 & 1 & 1 \\ 1 & 1 & -1 & -1 \\ 1 & -1 & 1 & -1 \\ 1 & -1 & -1 & 1 \end{pmatrix}, \tag{3.33}$$

and we note that it is the famous Hadamard matrix [42]. By the procedure known as the *Sylvester construction* [43], one can show that now we can find the matrices for higher N by a simple, recursive tensor product

$$A^{(N+1)} = A^{(1)} \otimes A^{(N)}. \tag{3.34}$$

Since the rows of Hadamard matrices are all mutually orthogonal and we use only at most $4^{N+1} - 1$ of them, we have now shown that there are infinitely many solutions to our problem and we have a significant freedom in their choice. We are later going to take advantage of this freedom to tailor the solutions to accommodate further requirements in the individual cases.

3.3.1 Algorithmic Solutions

From the previous sections follows that we are always able to find infinitely many solutions to the decoupling problem. Let us now write one explicitly and show how one can modify it with the freedom of infinitely many solutions.

Let us denote by $A^{(N+1)}_{\mathscr{J}}$ the matrix obtained from $A^{(N+1)}$ by taking only the subset of its rows $\mathscr{J}$. Now the system of linear equations can be written in matrix form

$$A^{(N+1)}_{\mathscr{J}}\vec{e} = \vec{r}, \qquad \vec{r} = \left(\frac{\nu_j}{\mu_j}\right)_{j\in\mathscr{J}}, \tag{3.35}$$

where $\vec{e}$ is the vector of unknown variables e_k.

The general procedure for solving systems of linear equations can now be applied. We split our solution into a particular solution and a solution of the corresponding

homogeneous system. A general solution is then the particular one plus one of the solutions of the homogeneous system.

The rows of Hadamard matrices $A^{(N+1)}$ are orthogonal and their norm is 4^{N+1},

$$A_j^{(N+1)} \cdot A_k^{(N+1)} = \delta_{j,k} 4^{N+1}. \tag{3.36}$$

From this it is now easy to write a particular solution

$$\vec{e}_r = \frac{1}{4^{N+1}} \left(A_{\mathscr{J}}^{(N+1)} \right)^T \cdot \vec{r}, \tag{3.37}$$

since

$$A_{\mathscr{J}}^{(N+1)} \cdot \left(A_{\mathscr{J}}^{(N+1)} \right)^T = 4^{N+1} \mathbb{I}_{|\mathscr{J}|}, \tag{3.38}$$

where $|\mathscr{J}|$ is the cardinality of $\mathscr{J}$.

A solution $\vec{e}_0$ of the homogeneous system

$$A_{\mathscr{J}}^{(N+1)} \vec{e}_0 = \vec{0}, \tag{3.39}$$

is easy to write again using the fact that the rows of Hadamard matrices are orthogonal and therefore a vector formed by linear combination from any row of the Hadamard matrix $A_j^{(N+1)}$ not present in $A_{\mathscr{J}}^{(N+1)}$ is a solution to the homogeneous system. Generally any linear combination of such vectors is a solution to the homogeneous system

$$\vec{e}_0 = \sum_{j \notin \mathscr{J}} \gamma_j \left(A_j^{(N+1)} \right)^T. \tag{3.40}$$

Finally we can now write the general solution as

$$\vec{e} = \vec{e}_0 + \vec{e}_r. \tag{3.41}$$

The last step for obtaining an algorithm for finding solutions is to obtain the natural numbers c_k. For c_k to be positive, e_k have to be positive as well. If we found $\vec{e}_r$ by the procedure above such that it has negative elements, since $0 \notin \mathscr{J}$, we can always add an arbitrary multiple of $\left(A_0^{(N+1)} \right)^T$ to our particular solution and make its elements positive. Just take $\gamma_0 = \min\{e_k\}$ and instead of $\vec{e}_r$ take $\vec{e}_r + \gamma_0 \left(A_0^{(N+1)} \right)^T$ and you will have a solution with all the elements positive, since

$$\left(A_0^{(N+1)} \right) = (1, \ldots, 1). \tag{3.42}$$

Finally to find m by the procedure given earlier and therefore the natural numbers c_k, it is required that the numbers $\frac{e_k}{D}$ be rational. This cannot be guaranteed in general as the particular solution can contain irrational numbers depending entirely on $\vec{r}$. Since Dynamical Decoupling is an approximate method, at this step we do not mind replacing $\frac{e_k}{D}$ by close-enough rational numbers.

3.3.2 Linear Programming

Linear programming is mentioned here because it turns out to be very useful and effective for finding decoupling schemes. In the previous sections we have shown that for any pair of H and H_{id} we are always able to find a solution. However the method does not guarantee the existence of a reasonably sized scheme nor does it say anything about the time scaling factor D. Both of these parameters have important practical implications and must be addressed to make the scheme workable. This is the moment where linear programming comes in.

Linear programming is a group of optimization algorithms that can be used to maximize or minimize a linear target function under constraints having the form of equalities or inequalities. Examples of algorithms include the Dantzig's Simplex algorithm, Ellipsoid algorithm, Criss-cross algorithm or the Projective algorithm [44]. In general linear programming requires the target function ϕ to be a real affine function, which is a more general class than linear functions. Lastly, linear programming assumes the optimization to be over a convex polytope.

Most frequently the problem is formulated as [45]

$$\begin{aligned} f(\vec{x}) &= \vec{c}^T\vec{x}, \\ A_{ub}\vec{x} &\leq \vec{b_{ub}}, \\ A_{eq}\vec{x} &= \vec{b_{eq}}, \\ \vec{lb} \leq \vec{x} &\leq \vec{ub}, \end{aligned} \tag{3.43}$$

where $\vec{x}$ are the independent variables, $\vec{c}$ is a real vector defining the affine target function f, A_{ub} and A_{eq} are matrices of inequality and equality constraints and $\vec{lb}$ and $\vec{ub}$ are vectors of lower and upper bounds respectively.

We can use linear programming for finding solutions to our problem while minimizing D. Just take the vector of variables and equality constraints from (3.35) and the target function to minimize to be the D from (3.30)

$$\begin{aligned} \vec{x} &\equiv \vec{e}, \\ A_{eq} &\equiv A^{(N+1)}, \\ (b_{eq})_j &\equiv \frac{\nu_j}{\mu_j},\ j \in 0 \ldots 4^{N+1} - 1, \\ f &\equiv D = \sum e_k, \\ \vec{lb} &\equiv \vec{0}. \end{aligned} \tag{3.44}$$

Any of the common algorithms will now give us a solution with minimal D. We still do not know anything about m. It turns out [46] that for most situations this is

sufficient. In cases where this is not true, one can always start with systems with a lower number of qubits and fallback on the freedom given by the homogeneous solution presented above and improve the scheme by hand. Another advantage of the linear programming procedure is that in practice some of the unitary pulses might be difficult to implement, thus being undesired in the scheme, and we can place further restrictions on the system of equations to eliminate them. Example of this are the σ^z pulses on trapped ions, which often excite the atoms and lead to losses from the trap.

Chapter 4

QST and Orthogonal Polynomials

Over the years the number of theoretical frameworks in which QST has appeared did grow enormous [1], the most recent one being orthogonal polynomials. We are going to use them in the upcoming sections as well, therefore an overview is in place. The idea to describe qubit chains with orthogonal polynomials first appeared in [8] and was further developed mainly in [6, 10]. Another reason for the review is that the framework of orthogonal polynomials allows us to show all the known properties of QST. The unique property of orthogonal polynomials when used to describe the qubit chains is that they allow to talk about more complicated structures than just linear chains. They allowed Christandl et al. and Miki et al. [6, 10] to give analytic solutions to the QST problem beyond the nearest neighbor chains for the first time.

4.1 Linear Structures

In the following we are going to show that one can construct qubit networks that can be used for QST in a very general context of multidimensional topological structures, but to get there, we first need to focus on the simplest cases of nearest-neighbor linear chains and build up from those.

4.1.1 Nearest Neighbor Chains

Even though in general we work with the Hamiltonians given by (2.2), let us for now focus on Hamiltonians of linear chains where only the closest neighbors are allowed to interact

$$H = \frac{1}{2}\sum_{i=0}^{N}\left[I_{i+1}\left(\sigma_i^x\sigma_{i+1}^x + \sigma_i^y\sigma_{i+1}^y\right) + B_i\left(\sigma_i^z + 1\right)\right]. \tag{4.1}$$

We will see later that this is at the core of computations for more complex structures. Since the Hamiltonian (2.2) preserves the total number of excitations as mentioned earlier, in order to achieve QST, we only need to focus on the subspace of single excitation, which is spanned by the basis vectors (2.16)

$$|i\rangle = (\underbrace{0,\ldots,0}_{i \text{ times}},1,0,\ldots,0),\ i=0,\ldots,N. \tag{4.2}$$

In this basis the Hamiltonian (4.1) has the matrix representation

$$H = \begin{pmatrix} B_0 & I_1 & 0 & & \\ I_1 & B_1 & I_2 & & \\ 0 & I_2 & B_2 & I_3 & \\ & & \ddots & \ddots & \\ & & & I_{N+1} & B_N \end{pmatrix}. \tag{4.3}$$

This is the moment where orthogonal polynomials come into the picture. We can write explicitly how this Hamiltonian acts on the basis vectors (2.16)

$$H\,|i\rangle = I_{i+1}\,|i+1\rangle + B_i\,|i\rangle + I_i\,|i-1\rangle\,, \tag{4.4}$$

and this with the natural additional constraints

$$I_0 = I_{N+2} = 0, \tag{4.5}$$

gives recurrence relations which look incredibly similar to the recurrence relations of orthogonal polynomials [47].

Because the matrix of H is Hermitian, there exist $N+1$ vectors such that

$$H\,|s\rangle = x_s\,|s\rangle\,,\ s=0,1,\ldots,N. \tag{4.6}$$

The eigenvalues x_s are real and furthermore, we restricted ourselves to strictly positive couplings and positive magnetic field strengths in Eq. (2.2). This means that the matrix (4.3) belongs to a class of tridiagonal matrices called *Jacobi matrices* and that the eigenvalues are non-degenerate [48, 49, 8]. Furthermore let us choose the labeling by s so that $x_0,\ldots,x_N$ form an increasing sequence.

The transition between the two bases can be written as:

$$|s\rangle = \sum_{i=0}^{N} V_i(s)\,|i\rangle\,, \tag{4.7}$$

with the inverse transformation given by

$$|i\rangle = \sum_{s=0}^{N} V_i(s) \, |s\rangle \, , \tag{4.8}$$

From (4.4) it can be seen that the expansion coefficients must satisfy

$$I_{i+1}V_{i+1}(s) + B_iV_i(s) + I_iV_{i-1}(s) = x_sV_i(s). \tag{4.9}$$

These 3-term recurrence relations, which by Favard's theorem [47], can be satisfied by polynomials $\chi_i(x)$

$$V_i(s) = V_0(s)\chi_i(x_s), \tag{4.10}$$

thus giving

$$I_{i+1}\chi_{i+1}(x) + B_i\chi_i(x) + I_i\chi_{i-1}(x) = x\chi_i(x), \tag{4.11}$$

with $\chi_0 = 1$ and $\chi_{-1} = 0$.

Since both bases are orthonormal, the following holds

$$\begin{aligned} \sum_i V_i(s)V_i(r) &= \delta_{s,r}, \\ \sum_s V_i(s)V_j(s) &= \delta_{i,j}. \end{aligned} \tag{4.12}$$

We now know that the polynomials $\chi_i(x)$ are orthogonal on the spectral points x_s

$$\sum_{s=0}^{N} V_0(s)^2\chi_i(x_s)\chi_j(x_s) = \delta_{i,j}. \tag{4.13}$$

Using this we can now rewrite the vector expansions as

$$|s\rangle = \sum_{i=0}^{N} V_0(s)\chi_i(x_s) \, |i\rangle \, , \tag{4.14}$$

and

$$|i\rangle = \sum_{s=0}^{N} V_0(s)\chi_i(x_s) \, |s\rangle \, . \tag{4.15}$$

From the right hand side of the recurrence relations (4.11) together with the initial conditions it follows that polynomials defined as

$$P_i(x) = I_1I_2 \ldots I_i\chi_i(x), \tag{4.16}$$

are actually monic polynomials

$$P_i(x) = x^i + O(x^{i-1}). \tag{4.17}$$

To give explicit formulas for constructing QST Hamiltonians it is preferable to work with these instead of $\chi_i(x)$.

$P_i(x)$ satisfy very similar recurrence relations as their counterparts $\chi_i(x)$, namely

$$P_{i+1}(x) + B_i P_i(x) + I_i^2 P_{i-1}(x) = x P_i x. \tag{4.18}$$

Again, these polynomials are orthogonal on the spectral points x_s

$$\sum_{s=0}^{N} P_i(x_s) P_j(x_s) V_0^2(s) = h_i \delta_{i,j}, \tag{4.19}$$

where

$$h_i = I_1^2 I_2^2 \dots I_i^2. \tag{4.20}$$

Since P_i defined by (4.16) have the same initial conditions as $\chi_i(x)$, namely

$$P_0 = 1,\ P_{-1} = 0, \tag{4.21}$$

deriving an explicit formula for P_{N+1} now becomes straightforward

$$P_{N+1}(x) = (x - x_0)(x - x_1) \dots (x - x_N). \tag{4.22}$$

It will come handy to express the weights in the orthogonality relations (4.19) using the common tricks of trade of orthogonal polynomials [47] as

$$V_0(s)^2 = \frac{h_N}{P_N(x_s) P'_{N+1}(x_s)},\ s = 0, \dots, N. \tag{4.23}$$

In order for state transfer to happen between sites i, k after time T, we require $F(T) = 1$ from (2.9), this can be rewritten to

$$\langle k | \, e^{-iTH} \, | i \rangle = e^{i\varphi}, \tag{4.24}$$

This equation can be expanded to

$$\sum_s V_i(s) \, \langle s | \, e^{-iTH} \sum_u V_k(u) \, | u \rangle = e^{i\varphi}, \tag{4.25}$$

which can be further simplified using the orthonormality of the basis eigen-vectors to

$$\sum_s V_i(s) V_k(s) e^{-iT x_s} = e^{i\varphi}. \tag{4.26}$$

for some φ. This will play an important part later when describing 2D structures.

We now focus on the procedure given in [8] of choosing coupling strengths and magnetic field strengths for achieving exactly this for the choice $i = 0$, $k = N$. In this case we require equivalently to (4.24)

$$e^{-iTH} |0\rangle = e^{i\varphi} |N\rangle , \tag{4.27}$$

we allow for an arbitrary fixed phase which in the worst case has to be corrected for. Let us expand this using (4.15) and the initial condition $\chi_0(x) = 1$ to see what this means for the polynomials $\chi_i(x)$

$$\chi_N(x_s) = e^{-i\varphi} e^{-iTx_s},\ s = 0, \ldots, N. \tag{4.28}$$

If we take a look at the recurrence relations and the initial conditions, we know that the polynomials $\chi_i(x)$ are real, therefore this relation is only possible if

$$\chi_N(x_s) = \pm 1, \tag{4.29}$$

which in turn is only possible if

$$\chi_N(x_s) = (-1)^{N+s}. \tag{4.30}$$

This follows from the increasing ordering of x_s, the famous *interlacing property* of orthogonal polynomials and the fact that

$$\begin{aligned} P'_{N+1}(x_s) &= (x_s - x_0)(x_s - x_1) \ldots (x_s - x_{s-1})(x_s - x_{s+1}) \ldots (x_s - x_N) \\ &= (-1)^{N+s} \left| P'_{N+1}(x_s) \right| . \end{aligned} \tag{4.31}$$

Now (4.30) and (4.28) are equivalent to

$$e^{-i\varphi} e^{-iTx_s} = e^{i\pi s} e^{i\pi N} e^{2i\pi L_s}, \tag{4.32}$$

where L_s are arbitrary integer numbers. If we now write the same relation for $s + 1$

$$e^{-i\varphi} e^{-iTx_{s+1}} = e^{i\pi(s+1)+} e^{i\pi N} e^{2i\pi L_{s+1}}, \tag{4.33}$$

and divide these two, we arrive at the necessary and sufficient condition for QST, the spacing of the eigenvalues of the respective Hamiltonian

$$x_{s+1} - x_s = \frac{\pi}{T} M_s, \tag{4.34}$$

where M_s are arbitrary positive odd numbers. This is yet another time we see that QST is essentially a condition on the spectrum of the Hamiltonian.

QST Hamiltonians are Persymmetric

The equation (4.30) can be further used to show an essential property of any QST Hamiltonian. Using the equations (4.31) and (4.23) it can be shown that it is equivalent to

$$V_0(s)^2 = \frac{I_1 \dots I_N}{\left|P'_{N+1}(x_s)\right|} > 0. \tag{4.35}$$

Let us now consider an additional *mirror* matrix

$$R = \begin{pmatrix} & & & 0 & 1 \\ & & & 1 & 0 \\ & & \dots & & \\ 0 & 1 & & & \\ 1 & 0 & & & \end{pmatrix}. \tag{4.36}$$

Since it is unitary, we can construct another Hamiltonian from (4.3) simply by

$$H^\star = RHR = \begin{pmatrix} B_0^\star & I_1^\star & 0 & & \\ I_1^\star & B_1^\star & I_2^\star & & \\ 0 & I_2^\star & B_2^\star & I_3^\star & \\ & & \ddots & \ddots & \\ & & & I_{N+1}^\star & B_N^\star \end{pmatrix}. \tag{4.37}$$

The coefficients now correspond to a situation where we have relabeled the qubits in our network

$$\begin{aligned} B_i^\star &= B_{N-i}, \\ I_i^\star &= I_{N-i}. \end{aligned} \tag{4.38}$$

For this Hamiltonian we can follow exactly the same procedure with orthogonal polynomials as before, since the Hamiltonians have the same spectra. The weights of these polynomials are different in general, but a beautiful relation can be found [50] between $V_0(s)^2$ and $V_0^\star(s)^2$

$$V_0(s)^2 V_0^\star(s)^2 = \frac{h_N}{\left(P'_{N+1}(x_s)\right)^2}. \tag{4.39}$$

Let us now consider the situation of $H = H^\star$ defined in (4.37). In this case the equation (4.39) tells us immediately that (4.35) automatically holds. This means that we have shown that if one takes a Hamiltonian with non-degenerate spectrum which is *persymmetric* ($H = H^\star$), the QST condition is fulfilled.

The equation (4.39) can be also used to show that the inverse is also true. Let us assume that we have a Hamiltonian which allows QST, hence we know that it leads to Eq. (4.35), which together with (4.39) immediately gives

$$V_0(s)^2 = V_0^\star(s)^2. \tag{4.40}$$

This condition is equivalent to the matrix being persymmetric. The persymmetry of the underlying matrix is a well know property of QST Hamiltonians [1, 5] and we will use it later as well, because it is a very strong requirement. It is sometimes called the *mirror symmetry*.

Reconstructing the Hamiltonians from Their Spectra

So far we have only shown what are the conditions on the Hamiltonians in order to achieve QST, we have not yet shown how to obtain the Hamiltonians once we choose the spectrum by fixing the freedom in (4.34).

Let us have the set of spectral points $\{x_s\}$, and we know the value the polynomial $\chi_N(x)$ takes on this set of points from (4.30). We are looking for a polynomial of degree N with $N+1$ given values. It is therefore uniquely defined and can be found by the famous *Lagrange interpolation* [47]. It is given by

$$\chi_N(x) = \sum_{s=0}^{N} (-1)^{N+s} \mathscr{L}(x), \tag{4.41}$$

where $\mathscr{L}(x)$ are the *Lagrange polynomials*

$$\mathscr{L}(x) = \prod_{i=0, i\neq s}^{N} \frac{x - x_i}{x_s - x_i}. \tag{4.42}$$

If we divide these by their leading coefficients, we arrive at the monic polynomials $P_N(x)$.

Recalling equation (4.22) we see that we already know two monic polynomials. From these we are looking to construct all the remaining $P_i(x)$ for $i = 1, 2, \ldots, N-1$.

The recurrence relations allow us to construct all the remaining polynomials $P_i(x)$ for $i = N-1, i = N-2, \ldots, i = 1$. To achieve this divide $P_{N+1}(x)$ by $P_N(x)$. After some relabeling one arrives at

$$P_{N+1}(x) = q_N(x) P_N(x) + R_{N-1}(x), \tag{4.43}$$

where $q_N(x) = x - \beta_N$ for some β_N and $R_{N-1}(x)$ denotes the remaining polynomial of degree $N-1$. Again, we can rewrite R_{N-1} using the corresponding monic polynomial Q_{N-1}

$$R_{N-1}(x) = \gamma_N Q_{N-1}(x). \tag{4.44}$$

Plugging the result of the division into the recurrence relations (4.18), we obtain

$$\begin{aligned} \beta_N &= B_N, \\ \gamma_N &= I_N^2, \\ Q_{N-1}(x) &= P_{N-1}(x). \end{aligned} \tag{4.45}$$

The last equation in (4.45) then defines P_{N-1}. We can iterate the same procedure to get P_{N-2} etc.

A special case of considerable importance for physicists is the case of $B_i = 0$ for all i, the case of zero magnetic fields. This case is easier to implement experimentally. In this case it can be shown [47]

$$P_i(-x) = (-1)^i P_i(x), \tag{4.46}$$

from which we can obtain, following the same logic as before, much more strict conditions on the spectrum and the weights of the corresponding orthogonal polynomials, namely

$$x_s = -x_{N-s}, \tag{4.47}$$

$$V_0(s)^2 = V_0(N-s)^2. \tag{4.48}$$

The second condition here is just a consequence of the first one. To see this let us assume that we have chosen the spectrum so that (4.34) holds and at the same time (4.47) holds. Calculating $V_0(s)^2$ from the left hand part of equation (4.35), we see that (4.48) holds as well. Thus in order to have Hamiltonians with no magnetic fields, all we need to add to the condition (4.34) is the Eq. (4.47).

Example of QST Hamiltonian

Using the tools presented above we are going to present the most widely used protocol for QST [1]. Let us choose

$$x_s = s - \frac{N}{2}. \tag{4.49}$$

Equation (4.34) holds for this choice with $T = \pi$ and $M_s = 1$.

From (4.31) we get

$$\begin{aligned} P'_{N+1}(x_s) &= \left(s - \frac{N}{2} + \frac{N}{2}\right)(s-1)\dots(1)(-1)(-2)(s-N) \\ \left|P'_{N+1}(x_s)\right| &= s!(N-s)!, \end{aligned} \tag{4.50}$$

Using (4.35) together with the normalization condition

$$\sum_s V_0(s)^2 = 1, \tag{4.51}$$

obtained from (4.12), we get

$$\sum_{s=0}^{N} \frac{\sqrt{h_N}}{s!(N-s)!} = 1. \tag{4.52}$$

Using the *Binomial theorem*

$$\sum_{s=0}^{N} \frac{N!}{s!(N-s)!} \left(\frac{1}{2}\right)^s \left(1-\frac{1}{2}\right)^{N-s} = 1, \tag{4.53}$$

we obtain

$$\sqrt{h_N} = N! \left(\frac{1}{2}\right)^N. \tag{4.54}$$

All this combined gives us the binomial distribution for the weights

$$V_0(s)^2 = \frac{N!}{s!(N-s)!} \left(\frac{1}{2}\right)^N. \tag{4.55}$$

These weights are know to yield the *normalized symmetric Krawtchouk polynomials* [10] as the monic polynomials $P_i(x)$. It is therefore possible to take their known coefficients and use them to get the magnetic field strengths and couplings in the Hamiltonian (4.1)

$$\begin{aligned} B_n &= 0, \\ I_n &= \frac{1}{2}\sqrt{n(N+1-n)}. \end{aligned} \tag{4.56}$$

The particular choice (4.56) corresponds as stated above to transfer time $T = \pi$ seconds. Since the Hamiltonian with this choice corresponds to zero magnetic field strengths, all the couplings can be scaled by some positive real number λ which will result in scaling of time, but nothing else will be affected. The choice

$$\begin{aligned} B_n &= 0, \\ I_n &= \frac{\lambda}{2}\sqrt{n(N+1-n)}, \end{aligned} \tag{4.57}$$

therefore leads to state transfer after time of $\frac{\pi}{\lambda}$ seconds instead. We get exactly the same result as in the Krawtchouk chain (2.20).

4.1.2 Joining Linear Chains

We have seen how to construct QST chains by combining QST graphs into their Cartesian products in 2.1.3. The procedure inherently required creating many new interaction terms and relied on uniform coupling strengths. A question naturally arises if it is

possible to connect two or more linear chains with non-uniform couplings with the QST property somehow to obtain a larger QST chain as well. The idea is reminiscent of creating blocks of qubits which could be combined to construct more complex structures of more intricate topology. We are only able to provide partial answers for the NN chains based on numerical simulations and perturbation theory of matrices.

Let H_1 and H_2 be Hamiltonians of linear chains with $(O+1)$ and $(P+1)$ qubits respectively, both nearest neighbor and capable of QST. We allow for an additional XY interaction to be inserted between the last qubit of the first chain and the first qubit of the second chain. That means we allow for Hamiltonians of the form

$$H = \begin{pmatrix} H_1 & E \\ E^\dagger & H_2 \end{pmatrix}, \tag{4.58}$$

where

$$E = \begin{pmatrix} 0 & & & \\ \vdots & & 0 & \\ 0 & & & \\ \gamma & 0 & \dots & 0 \end{pmatrix}, \tag{4.59}$$

and $\gamma \in \mathbb{R}^+$ denotes the additional interaction strength between the H_1 and H_2 chains. The Hamiltonians H_1 and H_2 are assumed to remain unmodified by the joining procedure.

We know from 4.1.1 that a QST chain has to be persymmetric, same for H_1 and H_2 since these are both QST chains. This immediately restricts the possibilities of joining chains to

$$\begin{aligned} H_1 &= H_2 \equiv H_0, \\ O &= P \equiv N. \end{aligned} \tag{4.60}$$

In other words, the persymmetry limits us to joining identical chains.

If the two chains are not identical, the low control procedure introduced in Sec. 2.1 offers no solutions and one would have to relax the assumptions we made to achieve QST. One such way which would work for identical chains as well, would of course be to wait until QST happens on the first chain, decouple the last qubit from the first chain and then couple it to the second one.

An example of successfully joining two chains together is the case of joining two identical chains of two qubits with an additional interaction. In this case we can calculate the additional interaction strength γ from (2.20) and consider it to be a special case of a 4-qubit chain.

The general case, however, is more complex. First let us discuss the common perturbation theory estimates of the spectra of the matrix (4.58). At first glance the matrix perturbation theory seems to be a perfect fit for this problem, since usually we would know the spectrum $\sigma(H_0)$ and the spectrum $\sigma(E)$ is easily calculated while disregarding multiplicities to be $\{0, \gamma\}$.

If we label the eigenvalues of H_0 in non-decreasing order (remember that H_0 is a Jacobi matrix and it has a non-degenerate spectrum [48, 49, 8]) to be

$$\sigma(H_0) = \lambda_0, \ldots, \lambda_{N+1}, \tag{4.61}$$

the eigevalues of H from Eq. (4.58) with $\gamma = 0$ are

$$\sigma\left(H(\gamma = 0)\right) = \lambda_0, \lambda_0, \ldots, \lambda_{N+1}, \lambda_{N+1} \equiv \tilde{\lambda}_0, \ldots \tilde{\lambda}_{2N+2}. \tag{4.62}$$

If we label by $\hat{\lambda}_0, \ldots \hat{\lambda}_{2N+2}$ the eigenvalues of $H(\gamma)$ for non-zero γ, the common perturbation theory [51, 52] gives us two estimates on their distance from Eq. (4.62). The first is

$$\left|\hat{\lambda}_i - \tilde{\lambda}_i\right| \leq ||E||_S \,, \tag{4.63}$$

where $||E||_S = \max\left(\sigma(E)\right) = \gamma$ is the spectral norm. This estimate becomes useful when $\gamma \to 0$, which leads to a degenerate spectrum. Since $\gamma = 0$ describes two decoupled chains, QST is impossible in this case.

The second common estimate is

$$\left|\hat{\lambda}_i - \tilde{\lambda}_i\right| \leq \frac{||E||_S^2}{\eta}, \tag{4.64}$$

where

$$\eta = \min_{\lambda_1 \in \sigma(H_1),\, \lambda_2 \in \sigma(H_2)} |\lambda_1 - \lambda_2| \,. \tag{4.65}$$

This estimate is divergent in our case, since $\eta = 0$ if $H_1 = H_2 = H_0$. Making an estimate on the spectrum of H in Eq. (4.58) is thus difficult and we employed numerical simulations to see if it is possible to join two identical chains that allow QST.

Specifically we took the couplings of the chain H_0 to be given by Eq. (2.20), which gave us the time of the first transfer T on the single chain. Let us define

$$f_m(\gamma) \equiv \max_{t \in [0, 10T]} (F(t, \gamma)), \tag{4.66}$$

where $F(t, \gamma)$ is the fidelity of QST calculated at time t for the joined chain from Eq. (4.58) and some specific choice of γ. In this notation $F(t, 0) = 0$ for any $t \in \mathbb{R}_0^+$.

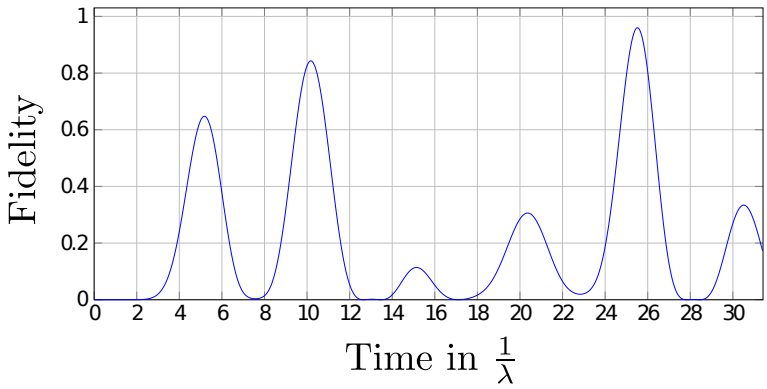

Figure 4.1: Fidelity in time (in $1/(\lambda)$ seconds), 8 qubit NNN chain composed of two identical 4-qubit QST chains (couplings from Eq. (2.20)), joined by an optimized interaction strength $\gamma = 0.73\lambda$. Notice a peak higher than 0.95 missing in the first half and the second peak rising to 0.96 in the second.

Essentially the function $f_m(\gamma)$ returns the maximum fidelity over ten QST intervals of the untethered chains.

We used L-BFGS-B optimization [53] to find γ which maximizes $f_m(\gamma)$. For the L-BFGS-B algorithm we bounded γ to a closed interval between 0 and two times the maximum coupling from Eq. (2.20)

$$0 \leq \gamma \leq 2 \max_i (I_{i,i+1}). \tag{4.67}$$

We applied this procedure for several configurations and numbers of qubits. Usually we were able to find γ such that f_m went above 0.95. However, increasing the resolution of the method and letting it iterate further never increased the maximum fidelity.

A representative case illustrating our findings is in Fig. 4.1 for 4 qubits ($N = 3$). Even though the second peak reaches 0.96, the overall behavior is much less regular than what we will see in later chapters in the simulations of the ideal case (Fig. 4.4). The answer to the question of whether it is possible to join two NN chains thus remains inconclusive (except for the requirements of two identical chains from persymmetry) as it seems to depend sensitively on the initial chain. Generally the joining does not lead to QST in a simple way and general approach is most probably impossible. However, in particular cases a QST solution could be found for example by the optimization described here.

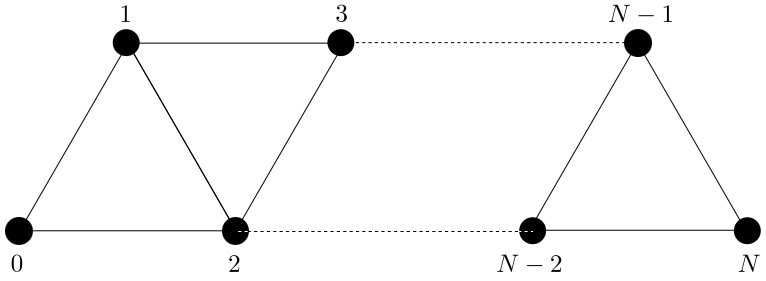

Figure 4.2: Next to nearest neighbor chain of an odd number of qubits (even N).

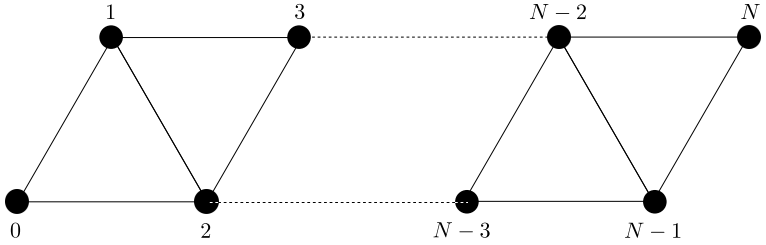

Figure 4.3: Next to nearest neighbor chain of an even number of qubits (odd N).

4.1.3 Next to Nearest Neighbor Chains

Most of the past research in QST on linear chains of qubits has been done on nearest neighbor chains [1]. Only recently analytic next to nearest neighbor protocols by Christandl et al. in [10] have been presented. While nearest neighbor couplings are certainly realistic and neglecting other interactions in the system is often justified by the physics underlying the system, next to nearest neighbor interactions cannot be ignored in a number of situations. For instance in more complex geometries or deformed geometries of originally nearest neighbor chains. We will occupy ourselves with perturbations to these next to nearest neighbor protocols in later sections, therefore we first want to give a brief overview of how they can be constructed.

Since the interactions between qubits are physical, it is conceivable that they depend on the spatial structure of the network. Next to nearest neighbor interactions then come in naturally as in Figures 4.2 and 4.3. The Hamiltonian, in this case, is given by

$$\begin{aligned} H &= \frac{1}{2}\sum_{i=0}^{N-1}\sum_{j=1}^{2} I_{i+j}^{(j)}\left(\sigma_i^x\sigma_{i+j}^x+\sigma_i^y\sigma_{i+j}^y\right) \\ &\quad +\frac{1}{2}\sum_{i=0}^{N} B_i\left(\sigma_i^z+1\right). \end{aligned} \tag{4.68}$$

If we denote by J the Hamiltonian (4.1) with the Krawtchouk couplings given by

(4.57), the main idea in [10] is to take

$$H = \alpha J^2 + \beta J. \tag{4.69}$$

Since the second degree polynomial of a tridiagonal matrix is a five diagonal matrix, if we could find α and β that allow for QST, we would have a NNN QST chain. In the case of $\alpha = 0$ we get the scaled couplings of the Krawtchouk chain again.

It has been shown that one can find infinitely many $\alpha > 0$ and $\beta \geq 0$ such that the NNN chain (4.68) supports QST. In fact it has been shown for J being any of the known Hamiltonians that lead to QST, but we restrict ourselves to the Krawtchouk case because it is the best understood. All the main points stem from the action of (4.68) on the computational basis (2.16)

$$\begin{aligned} H\left|i\right\rangle &= \alpha I_{i+1} I_{i+2} \left|i+2\right\rangle + \beta I_{i+1} \left|i+1\right\rangle \\ &\quad + \alpha (I_i^2 + I_{i+1}^2) \left|i\right\rangle + \beta I_i \left|i-1\right\rangle \\ &\quad + \alpha I_{i-1} I_i \left|i-2\right\rangle . \end{aligned} \tag{4.70}$$

This Hamiltonian differs in many respects and properties from the NN one (4.1). For example even for zero magnetic fields in J as in (4.57), the resulting magnetic fields in its quadratic polynomial (4.69) are given by

$$\tilde{B}_i = \alpha (I_i^2 + I_{i+1}^2), \tag{4.71}$$

which is nonzero if $\alpha \neq 0$. Furthermore the magnetic fields are dependent on i.

The most pronounced difference though is for $\beta = 0$. This eliminates all the nearest neighbor terms in (4.70). See Fig. 4.2, 4.3 to notice that this essentially splits the chains into two independent ones. Therefore no QST happens in the even case because the starting and target qubits belong to different unconnected chains.

Based on the results in [10], $\beta = 0$ is allowed only for odd number of qubits (even N) and state transfer is going to occur first at $T = \pi/(\lambda\alpha)$ and then periodically after $2\pi/(\lambda\alpha)$ for arbitrary α.

If $\beta > 0$, state transfer is going to occur only if α/β is some rational number

$$\frac{\alpha}{\beta} = \frac{p}{q}, \tag{4.72}$$

where p and q are two positive co-prime integers. If p is odd, q and N must have the same parity. For this choice of α and β QST is first going to happen at $T = \pi q/(\beta\lambda)$ and then periodically after $2\pi q/(\beta\lambda)$. As an example we plot the network's fidelity for 5 qubits and $\alpha = 2$, $\beta = 1$ in Fig. 4.4. Notice that $2/1$ is a rational number and p is even, the first arrival time appears at $T = \pi/\lambda$ seconds.

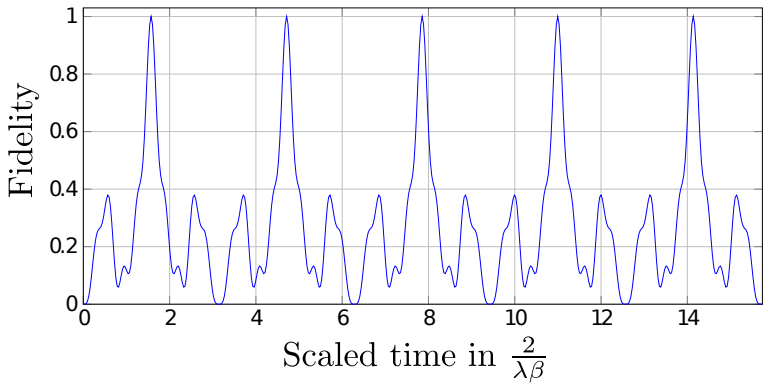

Figure 4.4: Fidelity of NNN chain with 5 qubits, $\alpha = 2$, $\beta = 1$ in time (in $(2/\beta\lambda)$). QST is achieved at $\pi/\beta\lambda$ seconds and then periodically after $2\pi/\beta\lambda$.

4.1.4 Relationship to QST on Graphs

Recently a peculiar connection of the Krawtchouk chains to QST on graphs has been discovered [14]. It turns out that the QST on the Krawtchouk chain can be directly viewed as a continuous time quantum random walk on a hypercube. Let us recall the notation of graphs from chapter 2.1.3.

In order to define a hypercube, let us consider a graph with vertices given by all the possible N-tuples of zeroes and ones, formally

$$V = \{0,1\}^N . \tag{4.73}$$

We use the Hamming distance to set the distance between two vertices $d(u,v)$. Between two vertices u and v we define $d(u,v)$ as the number of positions at which the two differ. Let us define for each $i \in \{0,\dots N\}$ a graph G_i as a graph with vertices (4.73) and edges between all the vertices that are in the Hamming distance i apart. G_1 is an N-dimensional hypercube.

If A_i is the adjacency matrix of G_i, define the intersection numbers $p^k_{i,j}$ as the number of vertices $z \in V$ such that

$$\begin{aligned} d(x,z) &= i, \\ d(y,z) &= j, \\ \text{for all } x,y \text{ such that } d(x,y) &= k. \end{aligned} \tag{4.74}$$

An interesting property of the adjacency matrices A_i is that they form the so called

Bose-Mesner algebra [14, 54]:

$$A_i A_j = \sum_{k=0}^{N} p_{i,j}^k A_k. \tag{4.75}$$

If we write this property for A_1, we get

$$A_1 A_i = (i+1)A_{i+1} + (N-i+1)A_{i-1}, \tag{4.76}$$

which can be viewed as recurrence relations implying

$$A_i = p_i(A_1), \tag{4.77}$$

where p_i is a polynomial of degree i. By a procedure very similar to how we have come the Krawtchouk polynomials from (4.55), one can show that $p_i(x)$ are again the Krawtchouk polynomials [54].

To establish the correspondence with QST in linear Krawtchouk chains, we need to write the time evolution of the graph G_1 as it was defined in (2.61), which is a continuous time quantum random walk on a hypercube

$$U(t) = e^{-itA_1}. \tag{4.78}$$

In order to write the action of this time evolution explicitly, we need to choose a basis in which to write the action of the matrix A_1. Let x_0 be the vertex made entirely of zeroes,

$$x_0 = (0, \ldots, 0), \tag{4.79}$$

and define V_n as a column vector of vertices from V by

$$V_n = \{x \in V | d(x_0, x) = n\}. \tag{4.80}$$

Each V_n is a vector of different length

$$|V_n| = k_n = \begin{pmatrix} N \\ n \end{pmatrix}, \tag{4.81}$$

with elements $V_{n,m}$, $m \in \{1, 2, \ldots, k_n\}$ which are N-tuples with exactly n ones. Since we defined G_1 to be a graph with edges between vertices with Hamming distance 1, each $V_{n,m}$ is connected to $N-n$ elements of the column V_{n+1} obtained by changing one 0 of $V_{n,m}$ to a 1.

Let us denote by $|x\rangle$ for each vertex $x \in V$ a vector from the standard basis of $\mathbb{C}^{|V|}$ chosen so that

$$\langle x|y\rangle = \begin{cases} 1 & \text{if } d(x,y) = 0 \\ 0 & \text{otherwise} \end{cases} \qquad (x, y \in V), \tag{4.82}$$

and by $|\text{col } n\rangle$ a vector obtained from the elements of V_n and their corresponding complex vectors as

$$|\text{col } n\rangle = \frac{1}{\sqrt{k_n}} \sum_{m=1}^{k_n} |V_{n,m}\rangle \,. \tag{4.83}$$

Calculation of the non-zero matrix elements of A_1 in the basis $|\text{col } n\rangle$ now gives

$$\begin{aligned} \langle \text{col } n+1 | \, A_1 \, | \text{col } n \rangle &= \frac{1}{\sqrt{k_n k_{n+1}}} \sum_{m=1}^{k_{n+1}} \sum_{o=1}^{k_n} \langle V_{n+1,m} | \, A_1 \, | V_{n,o} \rangle \\ &= \frac{k_n(N-n)}{\sqrt{k_n k_{n+1}}} = \sqrt{(n+1)(N-n)}. \end{aligned} \tag{4.84}$$

Since A_1 is symmetric, the following also holds true

$$\langle \text{col } n-1 | \, A_1 \, | \text{col } n \rangle = \langle \text{col } n | \, A_1 \, | \text{col } n-1 \rangle = \sqrt{n(N-n+1)}, \tag{4.85}$$

we can write the action of A_1 in the basis formed from the vectors $|\text{col } n\rangle$ to be

$$A_1 \, |\text{col } n\rangle = J_{n+1} \, |\text{col } n+1\rangle + J_n \, |\text{col } n-1\rangle \,, \tag{4.86}$$

where $J_n = \sqrt{n(N-n+1)}$.

It is exactly the same action as (4.4) with the Krawtchouk couplings (4.57) for $\lambda = 2$. Hence the systems are identical if we identify the vectors of the computational basis (3.15) with the column vectors $|\text{col } n\rangle$. For another, more complex example of projecting QST on a network of qubits onto a graph structure see [14], where an example with bivariate Krawtchouk polynomials can be found.

4.2 Two Dimensional Structures

In this chapter we are going to focus on two dimensional structures in which the qubits are placed on a rectangular lattice with a finite width $(M+1)$ and height $(N+1)$. It is then natural to label them with two indexes and expand the definition of the computational basis to

$$|i,j\rangle = \underbrace{\underbrace{|0\rangle \ldots |0\rangle}_{\text{width}\times i+j \text{ times}} \quad |1\rangle \, |0\rangle \ldots |0\rangle}_{\text{width}\times\text{height vectors}}, \text{ for } i = 0, \ldots N, \; j = 0, \ldots M. \tag{4.87}$$

We will show two examples of QST Hamiltonians on such a lattice. In chapter 4.2.1 we show a newly derived formalism for factorized 2D networks and then in 4.2.2 we present QST on a triangular lattice which was first described in [6].

4.2.1 QST on a Rectangular Lattice

Here we would like to show how to employ the 1D formalism to construct a 2D network that transfers state between arbitrary sites on a 2D rectangular lattice of qubits.

In a complete analogy to the 1D situation, let us index the sites with a tuple of integers $(i,j) = (0,\ldots,N;0,\ldots,M)$. Then the Hamiltonian can be written as

$$\begin{aligned} H &= \frac{1}{2}\sum_{i,j=0}^{N,M}\Big[I_{i+1,j}\left(\sigma_{ij}^x\sigma_{i+1,j}^x+\sigma_{ij}^y\sigma_{i+1,j}^y\right) \\ &\quad +J_{i,j+1}\left(\sigma_{i,j}^x\sigma_{i,j+1}^x+\sigma_{i,j}^y\sigma_{i,j+1}^y\right) \\ &\quad +B_{ij}\left(\sigma_{ij}^z+1\right)\Big], \end{aligned} \tag{4.88}$$

where I_{ij} are the horizontal couplings and J_{ij} are the vertical couplings between neighboring sites. This matrix is also Hermitian and therefore again its eigen-vectors $|s,t\rangle$ can be found, let us denote them

$$H|s,t\rangle = x_{st}|s,t\rangle. \tag{4.89}$$

The relations between the vectors $|s,t\rangle$ and $|i,j\rangle$ can again be written as

$$|s,t\rangle = \sum_{i,j} W_{i,j}(s,t)|i,j\rangle, \tag{4.90}$$

$$|i,j\rangle = \sum_{s,t} W_{i,j}(s,t)|s,t\rangle. \tag{4.91}$$

In complete analogy to (4.9), these expansion coefficients $W_{i,j}$ must satisfy

$$\begin{aligned} x_{st}W_{i,j}(s,t) &= I_{i+1,j}W_{i+1,j}(s,t)+J_{i,j+1}W_{i,j+1}(s,t) \\ &\quad +B_{ij}W_{i,j}(s,t)+I_{ij}W_{i-1,j}(s,t)+J_{ij}W_{i,j-1}(s,t). \end{aligned} \tag{4.92}$$

Let us assume that both these couplings were chosen so that I_{ij} are independent of j and similarly J_{ij} are independent of i. Let us further assume that not only the couplings I_{ij}, J_{ij}, but also the magnetic field strengths B_i and C_j have been chosen from equations of same form as (4.9), namely

$$I_{i+1,j}V_{i+1}(s)+B_iV_i(s)+I_{ij}V_{i-1}(s) = x_sV_i(s), \tag{4.93}$$

$$J_{i,j+1}W_{j+1}(t)+C_jW_j(t)+J_{ij}W_{j-1}(t) = y_tW_j(t). \tag{4.94}$$

Where $V_i(s)$ and $W_j(t)$ were calculated so that the two equations analogous to (4.26)

hold

$$\sum_s V_i(s)V_k(s)e^{-iTx_s} = e^{i\varphi}, \tag{4.95}$$

$$\sum_t W_j(t)W_l(t)e^{-iTy_t} = e^{i\eta}, \tag{4.96}$$

for some φ, η. Which can be done with exactly the same procedure as before. If we choose

$$\begin{aligned} W_{i,j}(s,t) &\equiv V_i(s)W_j(t), \\ B_{i,j} &\equiv B_i + C_j, \\ x_{st} &\equiv x_s + y_t, \end{aligned}$$

then the equation (4.92) holds as well.

More importantly, using the equations (4.95) and (4.96), and orthonormality of the basis vectors $|s,t\rangle$, we can show:

$$\begin{aligned} \langle i,j| e^{-iTH} |k,l\rangle &= \sum_{s,t} W_{ij}(s,t) \langle s,t| e^{-iTH} \sum_{u,v} W_{k,l}(u,v) |u,v\rangle \\ &= \sum_{s,t} W_{ij}(s,t)W_{kl}(s,t)e^{-iT(x_s+y_t)} \\ &= \sum_{s,t} V_i(s)W_j(t)V_k(s)W_l(t)e^{-iT(x_s+y_t)} \\ &= \underbrace{\sum_s V_i(s)V_k(s)e^{-iTx_s}}_{e^{i\varphi}} \underbrace{\sum_t W_j(t)W_l(t)e^{-iTy_t}}_{e^{i\eta}} \\ &= e^{i(\varphi+\eta)}. \end{aligned}$$

Therefore state transfer between the sites (i,j) and (j,k) and vise versa takes place. This is a novel way of constructing a 2D network of qubits which achieves QST.

4.2.2 Triangular Shape

Another example of a two dimensional structure that allows for QST is a triangular lattice, which is essentially a half of a square lattice N qubits wide split along the diagonal, with cleverly designed couplings and magnetic fields from [6] depicted in Fig. 4.5. Very similarly to QST on a lattice, the Hamiltonian for this case reads

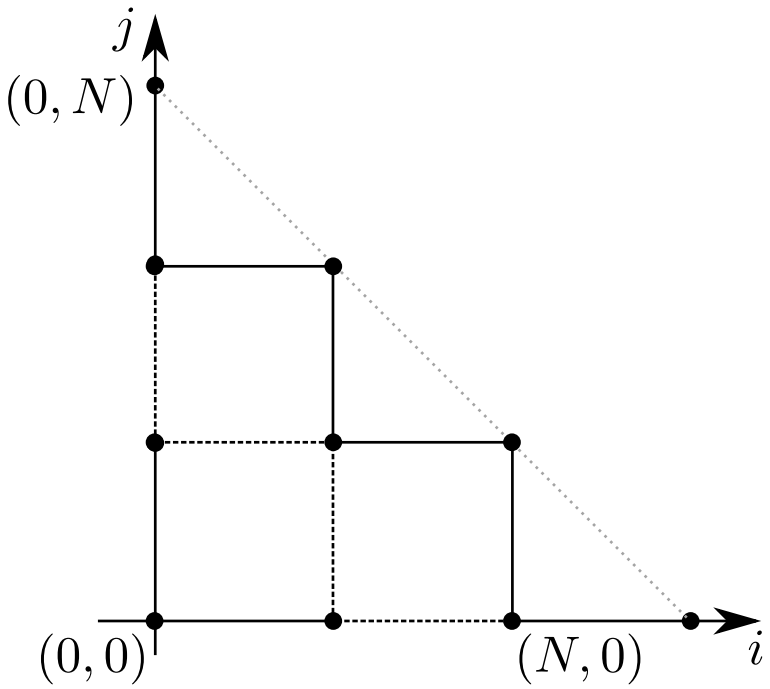

Figure 4.5: Triangular network of qubits.

$$\begin{aligned} H &= \frac{1}{2}\sum_{0\le i+j\le N}\Big[I_{i+1,j}\left(\sigma^x_{ij}\sigma^x_{i+1,j}+\sigma^y_{ij}\sigma^y_{i+1,j}\right) \\ &\quad +J_{i,j+1}\left(\sigma^x_{i,j}\sigma^x_{i,j+1}+\sigma^y_{i,j}\sigma^y_{i,j+1}\right) \\ &\quad +B_{ij}\left(\sigma^z_{ij}+1\right)\Big], \end{aligned} \tag{4.97}$$

where $I_{i+1,j}$ and $J_{i,j+1}$ have the boundary conditions $I_{0,j}=J_{i,0}=0$ and $I_{i+1,j}=J_{i,j+1}=0$ for $i+j\ge N$. Similarly to the previous case, let $|s,t\rangle$ be the eigenvectors corresponding to eigenvalues $x_{s,t}$:

$$H\,|s,t\rangle = x_{s,t}\,|s,t\rangle\,, \tag{4.98}$$

and let us expand them in the computational basis

$$|s,t\rangle = \sum_{0\le i+j\le N} W_{i,j}(s,t)\,|i,j\rangle\,. \tag{4.99}$$

This expansion is different from the one in Eq. (4.90) in that we cannot factorize it.

Plugging the expansion into the eigenvalue equation gives a five-term recurrence relation

$$x_{s,t}W_{i,j} = I_{i+1,j}W_{i+1,j} + J_{i,j+1}W_{i,j+1} + B_{i,j}W_{i,j} + I_{i,j}W_{i-1,j} + J_{i,j}W_{i,j-1}. \tag{4.100}$$

Inspired by the one dimensional case let us choose the couplings in two dimensions to be of a similar form

$$\begin{aligned} I_{i,j} &= \frac{1}{p_1+p_3}\sqrt{Sp_1p_3(p_2+p_4)i(N+1-i-j)}, \\ J_{i,j} &= -\frac{1}{p_2+p_4}\sqrt{Sp_2p_4(p_1+p_3)j(N+1-i-j)}, \\ B_{i,j} &= \frac{(N-i-j)S}{p_1p_4-p_2p_3}\left[\frac{p_2p_4(p_1+p_3)}{p_2+p_4}-\frac{p_1p_3(p_2+p_4)}{p_1+p_3}\right]+ \\ & \quad j\frac{p_1p_4-p_2p_3}{p_2+p_4}-i\frac{p_1p_4-p_2p_3}{p_1+p_3}, \end{aligned} \tag{4.101}$$

where $S=p_1+p_2+p_3+p_4$ and $p_1,p_2,p_3,p_4\in\mathbb{R}$.

Similarly to how we have arrived to the Krawtchouk chain, we choose

$$W_{i,j}=W_{0,0}(s,t)\frac{K_{i,j}(s,t)}{\sqrt{r_{i,j}}}, \tag{4.102}$$

where

$$r_{i,j}=\frac{(p_1p_4-p_2p_3)^{2(i+j)}S^{-(i+j)}}{(p_1p_3(p_2+p_4))^i(p_2p_4(p_1+p_3))^j}\begin{pmatrix} N \\ i,j \end{pmatrix}^{-1}, \tag{4.103}$$

with

$$\begin{pmatrix} N \\ i,j \end{pmatrix}=\frac{N!}{i!j!(N-i-j)!}, \tag{4.104}$$

being the trinomial distribution function and $K_{i,j}(s,t)$ is some yet unknown function of the indices.

Writing out the recurrence relations with these choices gives exactly the recurrence relations for the two-variate Krawtchouk polynomials $K_{i,j}(s,t)$ introduced in [55]. Similarly to previous considerations (Eq. (4.89)), the spectrum can be derived and in this case amounts to

$$x_{s,t}=(p_1+p_2)s-(p_3+p_4)t,\ 0\le s+t\le N. \tag{4.105}$$

The expressions for the two-variate Krawtchouk polynomials are known

$$K_{i,j}(s,t)=\sum_{0\le k+l+m+n\le N}\frac{(-i)_{k+l}(-j)_{m+n}(-s)_{k+m}(-t)_{l+n}}{k!l!m!n!(-N)_{k+l+m+n}}u_i^iv_1^ju_2^kv_2^l, \tag{4.106}$$

where

$$\begin{aligned} u_1 &= \frac{(p_1+p_2)(p_1+p_3)}{p_1 S}, \\ u_2 &= \frac{(p_1+p_2)(p_2+p_4)}{p_2 S}, \\ v_1 &= \frac{(p_1+p_3)(p_3+p_4)}{p_3 S}, \\ v_2 &= \frac{(p_2+p_4)(p_3+p_4)}{p_4 S}, \end{aligned} \tag{4.107}$$

and $(\alpha)_\beta = \alpha(\alpha+1)\dots(\alpha+\beta-1)$ are the Pochhammer symbols.

The eigenvectors $|s,t\rangle$ can be chosen to form an orthonormal basis, the same as the vectors in the computational basis, therefore the transition matrix with elements given by $W_{i,j}(s,t)$ is orthogonal. Since the weights with which the two-variate Krawtchouk polynomials are orthogonal on the spectral points, one can find

$$W_{0,0}(s,t) = \sqrt{\begin{pmatrix} N \\ s,t \end{pmatrix} \frac{1}{[(p_1+p_3)(p_2+p_4)]^N} \frac{(p_1p_4-p_2p_3)^{2(N-s-t)}(p_1p_2)^s(p_3p_4)^t}{(p_1+p_2)^{N-t}(p_3+p_4)^{N-s}}} \tag{4.108}$$

Because the transition matrix is orthogonal, the inverse relation holds as well

$$|i,j\rangle = \sum_{0\le s+t\le N} W_{i,j}(s,t)\,|s,t\rangle\,. \tag{4.109}$$

In general we have parametrized the couplings and magnetic field strengths by four real numbers, but to give a QST protocol we can restrict the parametrization to $p_1 = p_4$ and $p_2 = p_3$. If we denote $z = e^{-iT(p_1+p_2)}$, similarly to how we did it in chapter 4.1.1, we can write the fidelity of QST between sites (i,j) and (k,l) after time T to be

$$F_{(i,j),(k,l)}(T) = \left| \sum_{0\le s+t\le N} W_{i,j}(s,t) W_{k,l}(s,t) z^{s-t} \right|. \tag{4.110}$$

Using the tricks from [55] and choosing $(i,j) = (0,0)$, the fidelity becomes

$$\begin{aligned} F_{(0,0),(k,l)}(T) &= \left| \frac{\left[2p_1p_2(z-1)^2 + (p_1+p_2)^2 z\right]^{N-k-l}}{\sqrt{r_{k,l}}} \right. \\ &\quad \left. \cdot \frac{(p_1-p_2)^k (z-1)^{k+l} (p_2z+p_1)^k (p_1z+p_2)^l}{(p_2-p_1)^{-l} z^N (p_1+p_2)^{2N}} \right|. \end{aligned} \tag{4.111}$$

Now consider

$$T = \frac{\pi}{p_1+p_2}, \tag{4.112}$$

therefore $z = -1$ and the fidelity becomes

$$F_{(0,0),(k,l)}\left(\frac{\pi}{p_1+p_2}\right) = \sqrt{(2p_1p_2)^{k+l}\begin{pmatrix} N \\ k,l \end{pmatrix}}\frac{|p_1-p_2|^{(k+l)}}{(p_1+p_2)^{2N}}\left|8p_1p_2-(p_1+p_2)^2\right|^{N-k-l}. \tag{4.113}$$

If we restrict the freedom of the original parametrization one more time by requiring

$$(p_1+p_2)^2 = 8p_1p_2, \tag{4.114}$$

the fidelity becomes

$$F_{(0,0),(k,l)}\left(\frac{\pi}{p_1+p_2}\right) = \sqrt{(2p_1p_2)^{k+l}\begin{pmatrix} N \\ k,l \end{pmatrix}}\delta_{k+l,N}. \tag{4.115}$$

We have thus shown that the probability of QST occurring on the hypotenuse of the triangular network is given by a binomial distribution. Thus summing the square of the fidelity over all the indices on the hypotenuse gives

$$\sum_{k=0}^{N} F^2_{(0,0),(k,N-k)}\left(\frac{\pi}{p_1+p_2}\right) = 1. \tag{4.116}$$

Therefore we see QST happening between the starting vertex $(0,0)$ and the entire hypotenuse.

Furthermore it turns out that with the restrictions that we placed on p_1, p_2, p_3, p_4 the original parametrization of the couplings and magnetic field strengths simplifies to

$$\begin{aligned} \frac{I_{i,j}}{p_1+p_2} &= \frac{1}{2}\sqrt{i(N+1-i-j)}, \\ \frac{J_{i,j}}{p_1+p_2} &= \frac{-1}{2}\sqrt{j(N+1-i-j)}, \\ \frac{B_{i,j}}{p_1+p_2} &= \frac{p_1-p_2}{p_1+p_2}(j-i). \end{aligned} \tag{4.117}$$

This procedure is not a general method of constructing 2D structures, but it could nevertheless prove useful in some cases. It is easy to imagine this working as a logical bus topology for example. Even if one wants to consider QST on a rectangular lattice, this protocol offers a mean of QST between some sets of the qubits with a lower amount of control than for example sequential SWAP operations would.

Chapter 5

Perturbed Linear Chains

5.1 NN Chains

PST suffers from imperfections and the efficiency of transfer deteriorates. Parts of our results are centered around studies of several different perturbations to the networks presented in the previous chapters. The types of perturbations are inspired by realistic, natural physical character of the networks. The first such perturbation has been introduced in [11]. We will call it the *bent chain*. It is the simplest nearest neighbor chain with interactions given by Eq. (2.20) with one additional interaction. Fig. 5.1 shows a representative example of how this perturbation affects the network's performance. Without the bend the time evolution is periodic and the QST fidelity repeatedly reaches 1. With the additional interaction present even the first peak in fidelity drops significantly. It is realistic to imagine this as a result of a bend at site α, which would cause the neighboring qubits to become closer so that their interaction can no longer be neglected.

The additional interaction is assumed to have the same character as the interactions

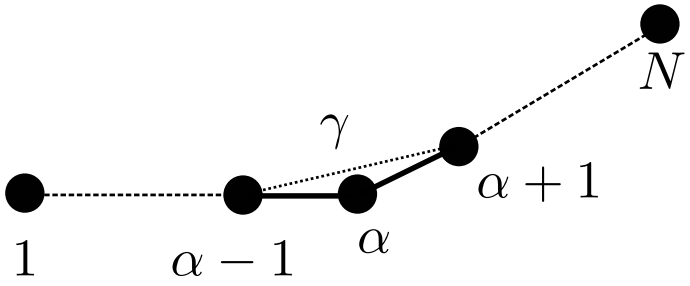

Figure 5.1: Bent nearest neighbor qubit chain with the resulting additional interaction.

in the unperturbed network and is hence of the form

$$H = H_{\mathrm{id}} + \gamma \left(\sigma^x_{\alpha-1}\sigma^x_{\alpha+1} + \sigma^y_{\alpha-1}\sigma^y_{\alpha+1} \right), \tag{5.1}$$

where H_{id} is given by Eq. (4.1), $\gamma \in \mathbb{R}^+$ and $\alpha \in [1, N]$. For the numerical experiments we always chose γ to be

$$\gamma = 0.4 \max \left\{ \frac{\lambda}{2}\sqrt{(\alpha-1)(N-\alpha+2)}, \frac{\lambda}{2}\sqrt{\alpha(N-\alpha+1)} \right\}. \tag{5.2}$$

This is a very representative case since the effects of the additional interaction do not show a heavy dependence on its position (except for the very edges) and are very similar once γ is roughly of the same order of magnitude as the largest coupling already in the network [11]. This coupling scales with the length of the chain in the same manner as the couplings (2.20), therefore it is always relatively as large as the largest coupling in the network.

The presence of this additional interaction has severe effects on the maximum achievable fidelity. In detail it has been explored in [11] also for a different choice of coupling strengths. Consequently it was explored in [7], where Dynamical Decoupling is the method of choice for correcting the effects of this additional interaction. For a representative case see Fig. 5.2. The additional interaction leads to the suppression of the first arriving peak, it further suppresses the following peaks and the read out time becomes less fault tolerant since some of the peaks are more narrow.

We will present several Dynamical Decoupling schemes that address this perturbation with numerical simulations that show their performance for various cases of Krawtchouk chains with couplings from Eq. (2.20) and γ from (5.2). The protocol (choice of couplings) is not the limiting factor here, all the schemes in the coming sections would work for any QST protocol.

5.1.1 Partial Dynamical Decoupling Scheme

Here we present a Dynamical Decoupling scheme that effectively removes the additional coupling but scales unevenly the two parts of the Hamiltonian (4.1). This is not a major issue since most usually the Krawtchouk chain is considered with zero magnetic fields. Furthermore, non-zero homogeneous magnetic fields $B_i = B$ only add a known phase which is easily accounted for [12]. We first commit on two approaches: solving the problem by hand and then by brute force numerical calculation.

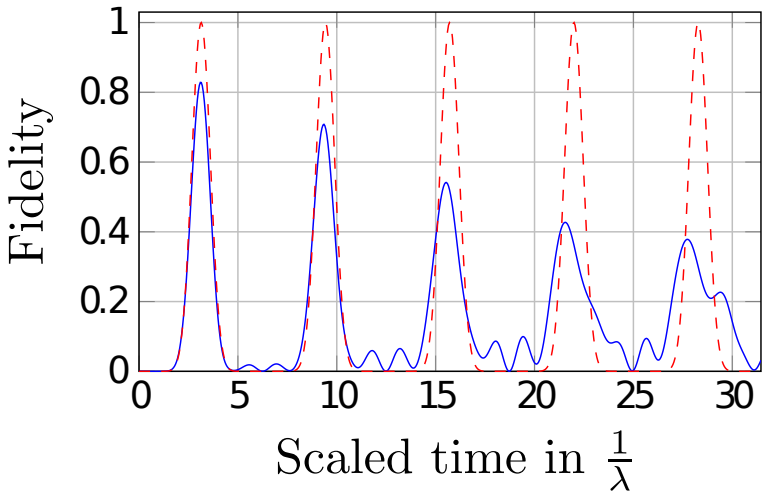

Figure 5.2: Fidelity in time (in $1/\lambda$ seconds), 10 qubit Krawtchouk chain. Red dashed line: $\gamma = 0$, blue solid line: γ as in (5.2). The quality of quantum state transfer is significantly suppressed as time progresses (blue line). Already the first transfer is below the benchmark value of 0.95

Solving by Hand

To further simplify equations (3.10), let us denote the recurring terms in the Hamiltonians by

$$h_{i,j} = \sigma_i^x \sigma_j^x + \sigma_i^y \sigma_j^y. \tag{5.3}$$

This immediately simplifies (4.1) and (5.1) to

$$H_{\text{id}} = \frac{1}{2} \sum_{i=0}^{N} \left[I_{i+1} h_{i,i+1} + B_i \left(\sigma_i^z + 1 \right) \right], \tag{5.4}$$

$$H = H_{\text{id}} + \gamma h_{\alpha-1,\alpha+1}. \tag{5.5}$$

If one tries to solve the main decoupling condition (3.10) by hand without using the algorithm from 3.3.1, the following property of $h_{i,j}$ often comes in handy

$$g^\dagger h_{i,j} g = -h_{i,j}. \tag{5.6}$$

Where $g = \sigma_i^z$ or $g = \sigma_j^z$. This relation is sometimes referred to as the *time reversal*.

The first step towards the partial decoupling scheme is to write out the expansion (3.8) for a specific choice of the scheme $\{g_0 = \mathbb{I}, g \equiv g_1 = \sigma_{\alpha-1}^z\}$

$$\overline{H}^{(0)} = \frac{1}{2}(H_{\text{id}} + g^\dagger H_{\text{id}} g + \gamma h_{\alpha-1,\alpha+1} - \gamma h_{\alpha-1,\alpha+1}) \tag{5.7}$$

$$= \frac{1}{2}(H_{\text{id}} + g^\dagger H_{\text{id}} g). \tag{5.8}$$

The additional interaction is now eliminated to the lowest order, however since $g^\dagger H_{\rm id} g \neq H_{\rm id}$, this is not a decoupling scheme yet, it needs further improvement.

Consider the scheme

$$\begin{aligned} g_0 &= \mathbb{I}, \\ g_1 &= \mathbb{I}, \\ g_2 &= \sigma_0^z \sigma_2^z \ldots \sigma_{\alpha-3}^z \sigma_{\alpha-1}^z, \\ g_3 &= \sigma_{\alpha+1}^z \sigma_{\alpha+3}^z \ldots \sigma_{N-1}^z \sigma_{N+1}^z, \end{aligned} \tag{5.9}$$

where g_2 applies σ^z to the qubit $\alpha - 1$ and every second qubit before it, while g_3 applies it to the qubit $\alpha + 1$ and every second qubit after it. g_2 acts as time reversal on all operators $h_{i,i+1}$ for $i < \alpha$ and $h_{\alpha-1,\alpha+1}$. Similarly, g_3 is the time reversal operator of $h_{i,i+1}$ for $i \geq \alpha$ and of $h_{\alpha-1,\alpha+1}$. This means that while all $h_{i,i+1}$ which are present in (5.4) have their sign reversed once, $h_{\alpha-1,\alpha+1}$ has it reversed by both g_2 and g_3. So writing out (3.8) for this scheme gives

$$\overline{H}^{(0)} = \frac{1}{2} \sum_{i=0}^{N} \left[\frac{1}{2} I_{i+1} h_{i,i+1} + B_i \left(\sigma_i^z + 1 \right) \right], \tag{5.10}$$

since g_i^z commutes with the magnetic part. This is equal to $\frac{1}{2} H_{\rm id}$ for $B_i = 0$. In the case of homogeneous magnetic fields $B_i = B$ this only means that the state to be transferred picks up additional relative phase of e^{2iBT} [7], which is easily corrected for. We call this procedure the *partial scheme*.

Numerical Simulations

Note the time scaling of $D = 2$ in Eq. (5.10). This means that if QST happened at some time T in the unperturbed case, in the perturbed case with Dynamical Decoupling it will happen at $2T$. We have run many simulations with different numbers of repetitions per π/λ seconds. We did not use the symmetrization trick in this case as the number of required pulses was very low already. For a representative result of different configurations see Fig. 5.3. We consistently managed to find a relatively small number of repetitions needed to make the first few peaks in fidelity go back to one (above 0.95) and restore the periodicity of the unperturbed protocol. By relatively small we mean tens of pulses per π seconds, experimental setups for dynamical decoupling operate in the regimes of thousands or tens of thousands pulses per π seconds [26].

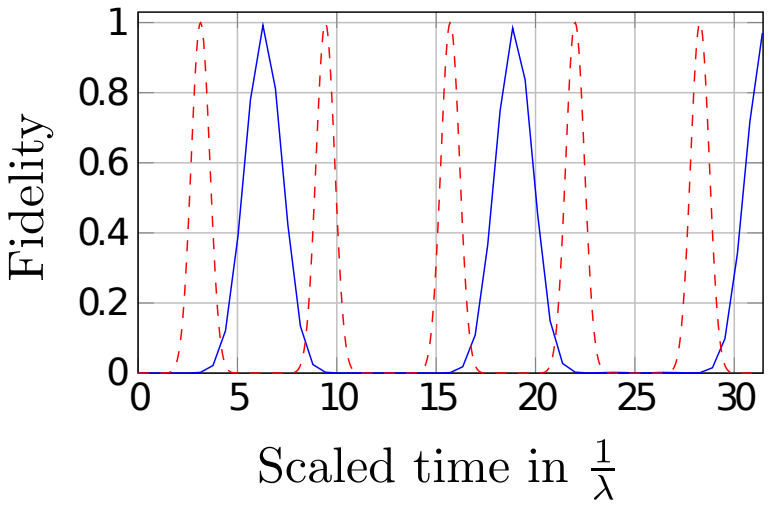

Figure 5.3: Fidelity in time (in $1/\lambda$ seconds), 10 qubit Krawtchouk chain with partial scheme applied. Red dashed line: $\gamma = 0$, blue solid line: γ as in (5.2), 5 repetitions of the partial scheme (20 pulses) per π/λ seconds. The peaks in fidelity come back close to one and perfect QST is restored (blue line), but the time is scaled by a factor of two compared to the ideal case (red line), leading to longer overall coherence times required.

5.1.2 Complete Decoupling Scheme

Solving Algorithmically

Here we present a scheme found by the procedures described in 3.3.1 and 3.3.2, we call it the *complete scheme*. Which means that this scheme minimizes the time scaling factor D. As it is the solution to the complete Eq. (3.10), the entire H_{id} is recovered. We ran the algorithmic procedures and got the following scheme with $m = 4$ operators

$$\begin{aligned} g_0 &= \mathbb{I}, \\ g_1 &= \sigma_0^x \sigma_1^x \dots \sigma_{\alpha-2}^x \sigma_{\alpha-1}^x, \\ g_2 &= \sigma_{\alpha+1}^y \sigma_{\alpha+2}^y \dots \sigma_{N-1}^y \sigma_N^y, \\ g_3 &= \sigma_1^z \sigma_3^z \dots \sigma_{\alpha-3}^z \sigma_{\alpha-1}^z \sigma_\alpha^x \sigma_{\alpha+2}^z \sigma_{\alpha+4}^z \dots \sigma_{N-2}^z \sigma_N^z. \end{aligned} \tag{5.11}$$

Similar to the Partial Decoupling Scheme, one could use the property (5.6) to verify the Eq. (3.10) by hand. This scheme works with $D = 2$. For a detailed step-by-step calculation see [7].

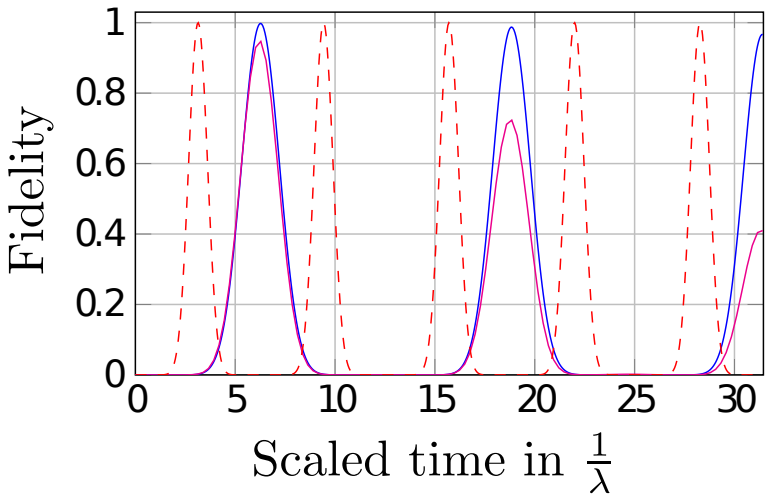

Figure 5.4: Fidelity in time (in $1/\lambda$ seconds), 10 qubit Krawtchouk chain with complete scheme applied. Red dashed line: $\gamma = 0$, magenta solid line: γ as in (5.2), complete scheme applied 12 times per π/λ seconds. Blue solid line: γ as in (5.2), complete scheme applied 60 times per π/λ seconds. Repeating the complete scheme more times per time unit (blue line) gives additional improvement compared to the lower number of repetitions (magenta line). At the same instant the overall improvement of QST is quite obvious.

Numerical Simulations

We carried out numerical simulations for various numbers of qubits in Krawtchouk chains, γ from (5.2) and α near the middle of the chain and were getting very consistent results. However this time we observed a significant drop in the number of required repetitions of the scheme per π/λ seconds once we used the symmetrization trick. Let us focus first on the case with no symmetrization.

For representative results in the number of qubits and numbers of repetitions see Fig. 5.4, where we plotted two different applications of the complete scheme with no symmetrization, one slower with 12 repetitions or 48 pulses per π/λ seconds, and second faster with 60 repetitions per π/λ or 240 pulses per π/λ seconds. It is apparent that while the first peak improves (above the set threshold only slightly - from $F \approx 0.947$ for 12 repetitions to $F =\approx 0.998$ for 60 repetitions) the increased number of pulses has significant influence on the later peaks where 60 repetitions recover above the tolerance level also these peaks.

For comparison we then used the symmetrization trick, the results are in Fig. 5.5.

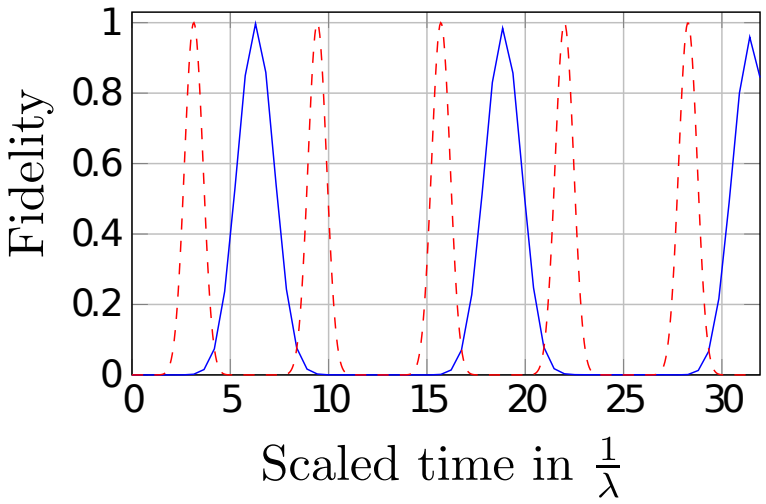

Figure 5.5: Fidelity in time (in $1/\lambda$ seconds), 10 qubit Krawtchouk chain with complete, symmetric scheme applied. Red dashed line: $\gamma = 0$, blue solid line: γ as in (5.2), complete symmetric scheme applied 12 times per π/λ seconds. Compare this Figure to Fig. 5.4 to see the significant improvement in performance when symmetrization is applied.

Compared to the above, once we employed the symmetrization trick, only 12 repetitions or 48 pulses per π/λ seconds were necessary to achieve improvement similar to 240 pulses before. Since higher number of pulses is always going to be more difficult to implement without disturbing the coherence of the system, keeping the repetition number low is of importance. The performance is comparable to the partial scheme, however this scheme does not introduce any additional relative phase, so it is not clear which would perform better in practice.

5.1.3 Practical Decoupling Scheme

Solving Algorithmically

We mentioned before that some of the unitary pulses might be undesired, such as the σ^z pulses, which are notoriously hard for the experimentalists to incorporate into their experiments. If that is the case, we present one additional decoupling scheme, we call it the *practical scheme* since it avoids the use of σ^z pulses. It was derived by hand from a scheme found by the presented algorithms but for H_{id} with no magnetic fields. In other words we asked not only for the additional interaction to be eliminated, but the magnetic fields as well. We then altered the found solution with the solution to the homogeneous

system (3.40) by hand to eliminate the σ^z pulses. The system of equations did not allow us to do that for the previous schemes.

The practical scheme is the following set of $m = 4$ unitary operators, $D = 2$

$$\begin{aligned} g_0 &= \mathbb{I}, \\ g_1 &= \sigma_0^x \sigma_1^x \dots \sigma_\alpha^x \sigma_{\alpha+1}^y \sigma_{\alpha+2}^x \sigma_{\alpha+3}^y \dots \sigma_N^x, \\ g_2 &= \mathbb{I}, \\ g_3 &= \sigma_0^y \sigma_1^x \sigma_2^y \dots \sigma_{\alpha-2}^x \sigma_{\alpha-1}^y \sigma_\alpha^x \sigma_{\alpha+1}^x \dots \sigma_N^x. \end{aligned} \tag{5.12}$$

The effective elimination of the magnetic fields results in an additional relative phase $e^{i\varphi} = (-i)^N$ added to the state transferred [7]. The elimination of the magnetic fields can also be viewed as an advantage of this particular scheme over the others. It is applicable not only to the case with additional coupling, but can also be used to correct for eventual inhomogeneous magnetic fields.

Numerical Simulations

We ran very similar simulations to the partial and complete schemes, a representative result without the symmetrization trick can be found in Fig. 5.6. We found that with no symmetrization the needed number of pulses (40 per π/λ seconds) lies between the partial and complete schemes. The result was the same for the symmetrized schemes, however the effect of symmetrization was most pronounced for the complete scheme. Typically the symmetrization lowered the number of required repetitions per π/λ seconds by one order for both the partial and practical schemes.

5.1.4 Limitations of Decoupling Schemes

Chain Length

One of the questions worth considering is the dependence of the required number of pulses on the number of qubits in the chain. This is an interesting topic since we know that the effect of the additional coupling tends to be less pronounced for longer chains than for short ones [11] suggesting a lower number of correction pulses needed. On the other hand, all the schemes require pulses to be applied to all the qubits in order to restore the desired dynamics. Stabilizing larger numbers of qubits could require a yet unspecified larger number of pulses per π seconds.

We sequentially increased the number of repetitions for the different schemes and different chain lengths until the fidelity of the first peak came above 0.95 and noted

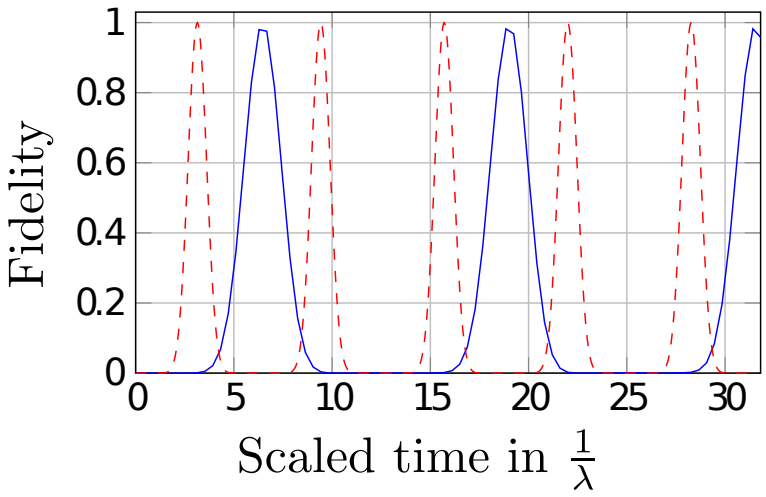

Figure 5.6: Fidelity in time (in $1/\lambda$ seconds), 10 qubit Krawtchouk chain with practical scheme applied. Red dashed line: $\gamma = 0$, blue solid line: γ as in (5.2), practical scheme applied 8 times per π/λ seconds. The protected time evolution (blue line) is again periodic and the peaks come back very close to one. The shift in time is cause by the applied correction method.

the required number of pulses. The results are in Fig. 5.7. For both the complete and practical schemes the required number of pulses seems to increase with the number of qubits in the chain while the partial scheme hovers around a constant number of 12, it can be again an increasing dependence, but with much lower increase. A more detailed study would require the study of longer chains which was beyond the accessible computational power.

Imperfect Pulses

Since we assume the additional interaction to stem from an imperfection, it was natural to ask ourselves what effect would it have if the pulses themselves in Dynamical Decoupling were implemented incorrectly. So we tested the schemes against Gaussian perturbations in timing of the pulses and against individual pulses being randomly rotated on the Bloch sphere to $\sigma^j e^{-i\theta\sigma^j}$ with θ sampled from a Gaussian distribution. Small perturbations seemed to have very little effect, but at a certain point became more pronounced. To be specific, the peaks of the fidelity did not significantly drop if the pulses happened between $\Delta T \pm 0.4\Delta T$ and were not rotated more than $\theta < 0.1\Delta T$.

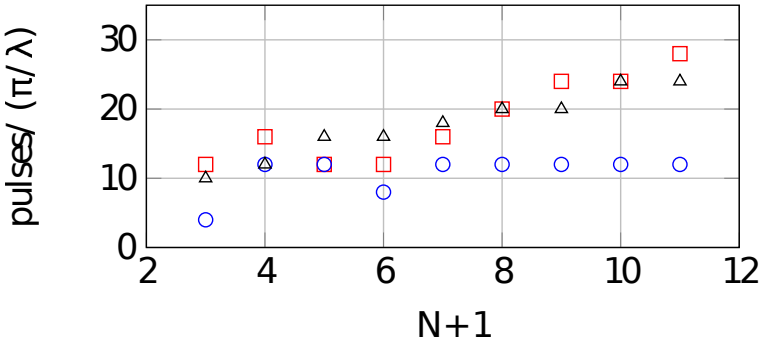

Figure 5.7: Minimal number of pulses required to make the first peak in fidelity larger than 0.95 for different numbers $N+1$ of qubits in the perturbed Krawtchouk chain, γ from (5.2) and α in the middle of the chain. Red squares: complete scheme with the symmetrization trick, blue circles: partial scheme, black triangles: practical scheme. Even if the dependence of the number of pulses on the chain length seems to grow for some schemes, it is nontrivial and based on the available data difficult to identify.

5.2 NNN Chains

Similarly to section 5.1, here we explore various realistic perturbations to the protocol from 4.1.3. Since every qubit in this protocol has at least two connections and the individual magnetic fields are always non zero, we are going to divide the perturbations into three categories. The first one will scale all the connections of one of the qubits, that corresponds to a similar situation to the bent chain. The second kind of perturbations modify a single coupling in the chain and the third modify one of the magnetic fields. For all the categories we give a way to construct a decoupling scheme that corrects for them together with numerical simulations of their performance. When we construct the schemes algorithmically, from now on we are always going to employ the symmetrization trick.

The main criterion for comparing individual decoupling schemes is the number of required pulses per π seconds for improving the first peak in fidelity above 0.95. The reason for this is the varying number of operators in each Dynamical Decoupling scheme, which causes the number of repetitions of the scheme per π seconds not to be comparable between the protocols. When we say that certain schemes perform similarly, we mean in the number of pulses per π seconds that bring the first peak in fidelity above 0.95.

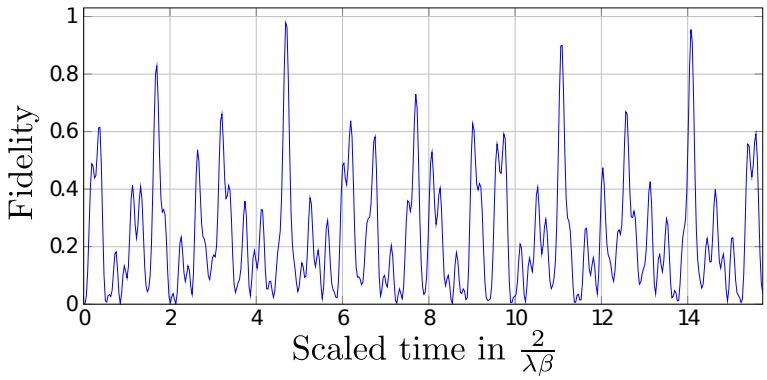

Figure 5.8: Fidelity in time (in $2/(\beta\lambda)$ seconds), 5 qubit NNN chain with all the couplings of the qubit $\mu = 2$ doubled. In the ideal case Fig. 4.4 the first peak appears at $\pi/\beta\lambda$, at this time we see a noticeable peak here as well, but is much lower and narrower. Overall the behavior is more irregular and although there are later peaks above 0.95, the first peak is the most significant one for QST. Furthermore, it is realistic to consider imperfect timing of the read-out operations as well and the peaks in fidelity are now much narrower leaving less space for timing errors.

5.2.1 Perturbing All Interactions of Qubits

This perturbation assumes a choice of one of the qubits $\mu \in \{0, \ldots, N\}$ for which all of its couplings have been multiplied by some $c > 0$. The procedures to find decoupling schemes are very different for the case of weakened couplings $c < 1$ and strengthened couplings $c > 1$ ($c = 1$ means there is no perturbation).

A very illustrative case is when all the couplings are doubled $c = 2$. The severe effect on the fidelity of the chain is in Fig. 5.8. The drop is most severe at the first peak and the behavior becomes significantly more irregular compared to the ideal case in Fig. 4.4.

To find a decoupling scheme that corrects for this, remember the time reversal property (5.6). Now consider the following decoupling scheme with $m = 4$

$$\begin{aligned} g_0 &= \sigma_\mu^z, \\ g_{1,2,3} &= \mathbb{I}. \end{aligned} \tag{5.13}$$

Now insert this into the lowest order approximation of the effective Hamiltonian obtained from Magnus expansion (3.8). Doubling the couplings for some μ means that the relevant interaction terms are present in the sum (4.68) twice. The operator g_0 acts as the time reversal operator on all the interactions of the qubit μ and does nothing to all the other

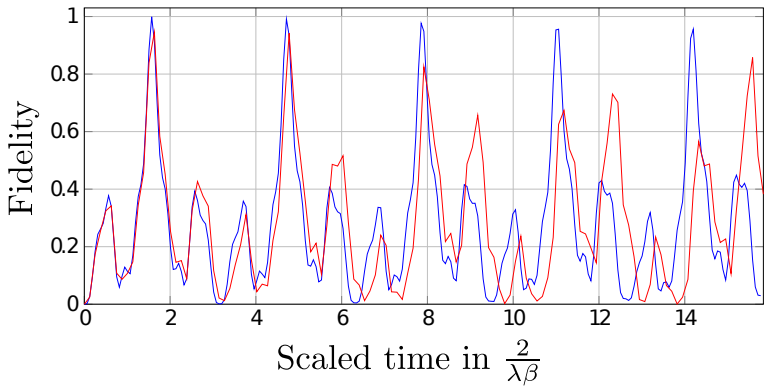

Figure 5.9: Fidelity in time (in $2/(\beta\lambda)$ seconds), 5 qubit NNN chain with all the couplings of the qubit $\mu = 2$ doubled. Blue line: protected with 400 pulses per $\pi/(\lambda\beta)$ seconds of the scheme (5.13), red line: protected with 200 pulses per $\pi/(\lambda\beta)$ seconds of the scheme (5.13). Both first peaks occur at nearly the same time and are very close to one, the following evolution is significantly protected by the scheme with more pulses (blue line).

terms. Therefore in the expansion they appear 4 times, but the sum is divided by four. Therefore to the lowest order the perturbation is eliminated with no time scaling $D = 1$. The performance of the scheme is plotted in Fig. 5.9, for both cases the first peak in fidelity comes back close to 1 and the overall shape is much more reminiscent of the ideal case presented in Fig. 4.4.

Coming up with a scheme for some other $c > 1$ essentially boils down to number theory. If c is not a rational number, let $\frac{r}{s}$ be its sufficient rational approximation. Since simulating the performance of a scheme is straightforward, finding the sufficient rational approximation becomes an iterative process of increasing the approximation accuracy until the scheme performs in simulations as desired. If c is rational, let $c = \frac{r}{s}$, where r and s are coprime integers and $r > s > 0$. Let e be the number of identities in the scheme and f the number of σ_μ^z pulses in the scheme. Writing out (3.10) gives

$$\frac{e+f}{e-f} = \frac{r}{s}. \tag{5.14}$$

This is one equation for two variables, but naturally we look for the lowest possible f. We can check the case of $c = 2$, in this case $r = 2$, $s = 1$ and (5.14) gives

$$\frac{e+f}{e-f} = 2. \tag{5.15}$$

Solving for lowest f gives $e = 3$, $f = 1$.

The cases with $c < 1$ are difficult to solve by hand, because the schemes must involve all the other qubits in the network. Therefore solving (3.10) in this case completely relies on the algorithms from 3.3.1 and 3.3.2. We applied those for multiple choices of μ and c and most of the time the resulting schemes were characterized by $D > 2$ and m in the lower hundreds, roughly 1/2 of them were identities. The resulting schemes showed heavy dependence on N in the sense of different operators employed.

For example we applied the algorithms for 5 qubits ($N = 4$), $c = 0.6$, $\alpha = 2$, $\beta = 1$ and $\mu = 2$. The result is

$$\begin{aligned} g_{0\ldots49} &= I, & g_{50} &= \sigma_3^y, \\ g_{51} &= \sigma_1^x\sigma_4^x, & g_{52\ldots57} &= \sigma_1^x\sigma_2^x\sigma_3^x, \\ g_{58\ldots59} &= \sigma_1^y\sigma_4^y, & g_{60\ldots67} &= \sigma_1^y\sigma_2^y\sigma_3^x\sigma_4^y, \\ g_{68\ldots69} &= \sigma_2^z, & g_{70\ldots74} &= \sigma_0^x\sigma_3^x\sigma_4^y, \\ g_{75\ldots79} &= \sigma_0^x\sigma_2^x\sigma_3^z\sigma_4^x, & g_{80} &= \sigma_0^x\sigma_1^x\sigma_2^x\sigma_4^z, \\ g_{81} &= \sigma_0^x\sigma_1^x\sigma_2^x\sigma_3^x\sigma_4^x, & g_{82\ldots84} &= \sigma_0^x\sigma_2^y, \\ g_{85\ldots90} &= \sigma_0^x\sigma_1^y\sigma_2^z\sigma_3^z\sigma_4^x, & g_{91\ldots97} &= \sigma_0^x\sigma_1^z\sigma_2^x\sigma_3^x, \end{aligned} \tag{5.16}$$

This is a decoupling scheme with $m = 98$ and $D = 7/3$. Fig. 5.10 shows its performance using numerical simulation. The number of pulses required is much higher in this case compared to the other schemes which might hinder its significance, but the first peak is restored almost entirely. Notice how it scales time compared to the ideal case. Because $D = \frac{7}{3}$, the first peak arrives in more than twice the time it takes for the unperturbed chain, but it is several times higher than in the perturbed case.

5.2.2 Perturbing One Interaction

The second kind of perturbations only disturbs one interaction strength in Eq. (4.68). We parametrize which $I_{i+j}^{(j)}$ is perturbed by $\mu \in \{0, \ldots, N\}$ and a $\nu \in \{1, 2\}$, resulting in the specific choice $I_{\mu+\nu}^{(\nu)}$. This coupling is multiplied by a scaling constant $c > 0$ to become $cI_{\mu+\nu}^{(\nu)}$. This time both the strengthening $c > 1$ and weakening $c < 1$ are addressed by running the algorithms described in 3.3.1 and 3.3.2.

The effects of this perturbation are less pronounced than in 5.2.1, which is not surprising since the perturbed Hamiltonian is much closer to the ideal one than before (Fig. 5.11). We give two examples of the solutions found algorithmically. Both for a 5 qubit NNN chain ($N = 4$), $\alpha = 2, \beta = 1$, $\mu = 2, \nu = 1$, but one for $c = 2$ and another one for

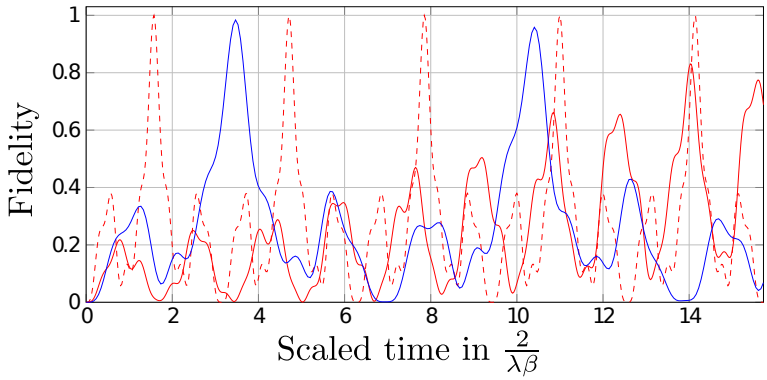

Figure 5.10: Fidelity in time (in $2/(\beta\lambda)$ seconds), 5 qubit NNN chain with all the couplings of the qubit $\mu = 2$ scaled by $c = 0.6$. Blue solid line: protected with 10000 pulses per $\pi/(\lambda\beta)$ seconds of the scheme (5.16), red solid line: unprotected, red dashed line: ideal case ($c = 1$). The perturbation has a pronounced deteriorating effect on the time evolution (red solid line compared to the red dashed line). The red solid peaks are lower and none of them reach the fidelity of 0.95. The first four peaks stay below the fidelity of 0.4 while the red dashed line reaches 1.0 two times in the same time frame. The evolution is restored and scaled when protected by the decoupling scheme (blue line).

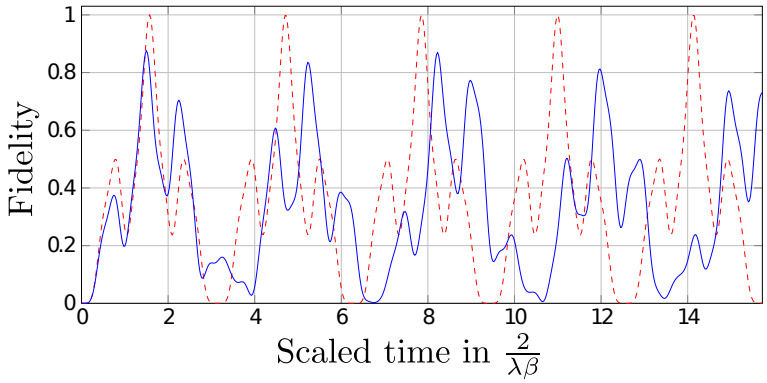

Figure 5.11: Fidelity in time (in $2/(\beta\lambda)$ seconds), 6 qubit NNN chain, $\alpha = 1, \beta = 1$ with one coupling of the qubit $\mu = 3, \nu = 1$ scaled by $c = 1.7$. Blue solid line: unprotected, red dashed line: ideal case ($c = 1$). Both the maximal value of fidelity and the time of QST are perturbed by the scaled interaction (blue line) compared to the ideal case (red dashed line).

$c = 10/13$. The solution for $c = 2$ is as follows

$$\begin{aligned} g_{0\ldots510} &= I, & g_{511\ldots553} &= \sigma_3^z, \\ g_{534\ldots539} &= \sigma_2^y\sigma_2^x\sigma_3^x, & g_{540\ldots569} &= \sigma_2^z, \\ g_{570\ldots606} &= \sigma_1^x\sigma_3^z\sigma_4^x, & g_{607\ldots636} &= \sigma_1^x\sigma_2^x\sigma_3^z\sigma_4^z, \\ g_{637} &= \sigma_1^x\sigma_2^z\sigma_3^x\sigma_4^z, & g_{638\ldots661} &= \sigma_1^y\sigma_2^x\sigma_3^y\sigma_4^z, \\ g_{662\ldots664} &= \sigma_1^y\sigma_2^z\sigma_3^y\sigma_4^y, & g_{665\ldots699} &= \sigma_1^z\sigma_2^y\sigma_3^z\sigma_4^y, \\ g_{700\ldots726} &= \sigma_0^x\sigma_3^x, & g_{727\ldots741} &= \sigma_0^x\sigma_1^x\sigma_2^y\sigma_3^x\sigma_4^y, \\ g_{742\ldots761} &= \sigma_0^x\sigma_1^x\sigma_2^z, & g_{762\ldots795} &= \sigma_0^x\sigma_1^x\sigma_3^z\sigma_4^x, \\ g_{796\ldots829} &= \sigma_0^x\sigma_1^z\sigma_2^x\sigma_3^y, & g_{830\ldots863} &= \sigma_0^x\sigma_1^z\sigma_2^z\sigma_3^x\sigma_4^x, \end{aligned} \tag{5.17}$$

it is a solution with $m = 864$ and $D = \frac{3}{2}$.

Applying the linear programming procedure for $c = \frac{10}{13}$ returns

$$\begin{aligned} g_{0\ldots78} &= I, & g_{79\ldots81} &= \sigma_2^x\sigma_3^x\sigma_4^y, \\ g_{82\ldots83} &= \sigma_1^x\sigma_2^x\sigma_3^x\sigma_4^z, & g_{84\ldots85} &= \sigma_1^x\sigma_2^z\sigma_3^z\sigma_4^y, \\ g_{86} &= \sigma_1^y\sigma_4^z, & g_{87} &= \sigma_1^y\sigma_2^x\sigma_3^x\sigma_4^x, \\ g_{88\ldots89} &= \sigma_1^y\sigma_2^y\sigma_3^y, & g_{90\ldots91} &= \sigma_1^z\sigma_2^z\sigma_3^z\sigma_4^z, \\ g_{92\ldots95} &= \sigma_0^x\sigma_2^z\sigma_3^z\sigma_4^x, & g_{96\ldots97} &= \sigma_0^x\sigma_1^x, \\ g_{98\ldots99} &= \sigma_0^x\sigma_1^y\sigma_2^z\sigma_3^z\sigma_4^y, & g_{100\ldots103} &= \sigma_0^x\sigma_1^z\sigma_2^x\sigma_3^x, \end{aligned} \tag{5.18}$$

which is a decoupling scheme with $m = 104$ and $D = \frac{13}{10}$. The fidelity with this scheme is in Fig. 5.12. The first peak comes back to 1, but overall the number of pulses for this scheme was much higher than for other schemes. A peculiar property in the cases of $c < 1$ is that the scaling of the automatically found solutions was always $D = 1/c$, not so for $c > 1$. However we are not able to prove this analytically due to the complicated nature of the schemes like (5.18).

5.2.3 Perturbations in the Magnetic Field

The third category of perturbations we explore are the perturbations of one of the magnetic fields labeled by $\mu \in \{0, \ldots, N\}$. The magnetic field strengths correspond to the diagonal elements in (4.70). Again we change one of the variables from (4.71) to $c\tilde{B}_\mu$, $c > 0$. The NNN Krawtchouk protocol seems to be very sensitive to the changes in magnetic fields, see Fig. 5.13, the effects are very similar for both $c > 1$ and $c < 1$. Again we rely on algorithmic solutions to find Dynamical Decoupling schemes to correct for these perturbations.

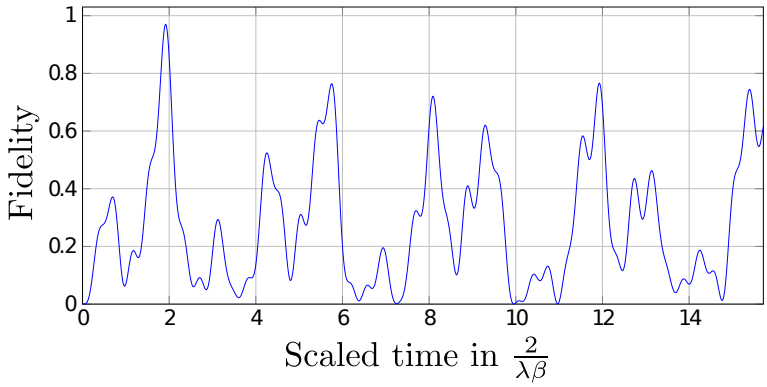

Figure 5.12: Fidelity in time (in $2/(\beta\lambda)$ seconds), 5 qubit NNN chain, $\alpha = 2, \beta = 1$ with one coupling of the qubit $\mu = 2, \nu = 1$ scaled by $c = 10/13$, protected by 50000 pulses per $\pi/(\lambda\beta)$ seconds of the scheme (5.18). The first peak in fidelity comes back above 0.95 and is useful for QST.

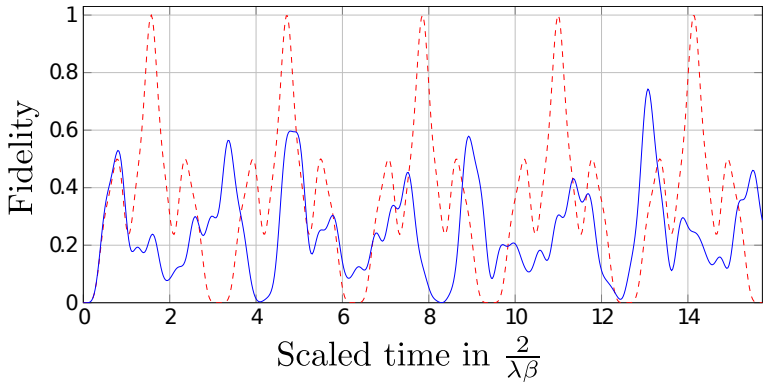

Figure 5.13: Fidelity in time (in $2/(\beta\lambda)$ seconds), 6 qubit NNN chain, $\alpha = 1, \beta = 1$ with one magnetic field $\mu = 3$ scaled by $c = 1/2$. Blue solid line: unprotected, red dashed line: ideal case. The fidelity of QST is severely affected and QST is lost completely by the scaled magnetic field (blue line) compared to the ideal case (red dashed line).

In contrast to the effects being similar for $c > 1$ and $c < 1$, the respective decoupling schemes vary for the two cases. Perturbations with $c > 1$ characteristically lead to lower scaling in time ($D < 2$) and lower number of operators in the scheme m, while $c < 1$ characteristically leads to $D > 2$ and higher number of operators in the scheme m.

A representative case for $c > 1$ is the scheme for 5 qubit NNN chain, $\alpha = 2, \beta = 1$, $\mu = 2$ and $c = \frac{5}{3}$ which is corrected by the scheme

$$\begin{aligned} g_{0\ldots17} &= I, & g_{18} &= \sigma_2^x\sigma_3^x\sigma_4^z, \\ g_{19} &= \sigma_2^y, & g_{20} &= \sigma_1^x\sigma_2^x\sigma_3^x\sigma_4^x, \\ g_{21} &= \sigma_1^z\sigma_2^x\sigma_4^x, & g_{22} &= \sigma_0^x\sigma_2^x, \\ g_{23} &= \sigma_0^x\sigma_1^x\sigma_2^x\sigma_3^z. \end{aligned} \tag{5.19}$$

It almost does not scale time with $D = \frac{6}{5}$ and has a low number of operators $m = 24$. On the other hand $c = \frac{3}{5}$ is corrected by

$$\begin{aligned} g_{0\ldots582} &= I, & g_{533\ldots590} &= \sigma_2^z\sigma_4^y, \\ g_{591\ldots614} &= \sigma_2^z\sigma_3^z\sigma_4^x, & g_{615\ldots650} &= \sigma_1^x\sigma_3^y, \\ g_{651\ldots686} &= \sigma_1^x\sigma_2^z\sigma_3^z\sigma_4^y, & g_{687\ldots723} &= \sigma_1^y\sigma_3^z\sigma_4^y, \\ g_{724\ldots725} &= \sigma_1^y\sigma_2^z\sigma_3^z, & g_{726\ldots748} &= \sigma_1^z\sigma_3^x\sigma_4^z, \\ g_{749\ldots775} &= \sigma_1^z\sigma_2^z\sigma_3^y\sigma_3^z, & g_{776\ldots809} &= \sigma_0^x\sigma_4^z, \\ g_{810\ldots814} &= \sigma_0^x\sigma_2^z\sigma_3^x, & g_{815\ldots840} &= \sigma_0^x\sigma_1^x\sigma_3^y\sigma_4^y, \\ g_{841\ldots850} &= \sigma_0^x\sigma_1^x\sigma_2^z\sigma_3^x\sigma_4^x, & g_{851\ldots864} &= \sigma_0^x\sigma_1^x\sigma_2^z\sigma_3^y, \\ g_{865\ldots897} &= \sigma_0^x\sigma_1^x\sigma_2^z\sigma_3^y\sigma_4^y, & g_{898\ldots901} &= \sigma_0^x\sigma_1^z\sigma_3^y\sigma_4^x, \\ g_{902\ldots934} &= \sigma_0^x\sigma_1^z\sigma_3^z, & g_{935\ldots953} &= \sigma_0^x\sigma_1^z\sigma_2^z, \\ g_{954\ldots969} &= \sigma_0^x\sigma_1^z\sigma_2^z\sigma_3^x\sigma_4^y, \end{aligned} \tag{5.20}$$

which involves $m = 970$ operators and scales time with $D = \frac{5}{3}$.

We experimented with different choices of the parameters α, β and numbers of qubits in the chain. If we fixed the scaling factor and number of qubits in the chain, the schemes we found for various α, β performed very similarly in the number of required pulses for the first peak in fidelity to come above 0.95. A representative example can be found in Fig. 5.14, in all the simulated configurations if the scheme brought the first peak above 0.95, the same was not true for the following peaks. In order to restore the periodic behavior as well, the number of required pulses was roughly five times higher.

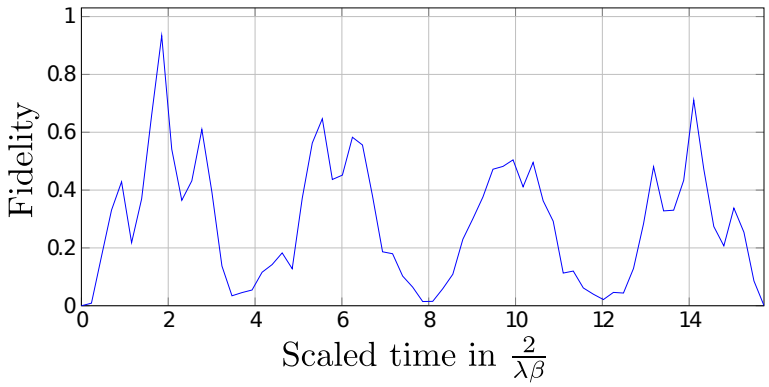

Figure 5.14: Fidelity in time (in $2/(\beta\lambda)$ seconds), 6 qubit NNN chain, $\alpha = 1, \beta = 1$ with one magnetic field $\mu = 3$ scaled by $c = 1.6$, protected by 5000 pulses per $\pi/(\beta\lambda)$ seconds of algorithmically found scheme. The first peak in fidelity is back above 0.95.

5.2.4 Comparing Perturbations of NNN Chains

The considered perturbations were all inspired by realistic physical considerations, but their characters and effects are very different. The perturbation of all of a qubit's interactions naturally affects the dynamics of a larger part of the network and thus even a scaling factor close to (but different from) 1 has a pronounced effect. Compared to that, in order to see similar effects on the first peak in fidelity, the scaling of a single coupling has to be roughly twice as far from 1 for the same network. In contrast even though the considered change in magnetic field affects only a single qubit, a small distance from 1 of the scaling factor of the magnetic field has adverse effects on the first peak in fidelity.

In the NNN case we had two families of couplings to choose from for the perturbation, the NN couplings and the beyond nearest neighbor couplings. Surprisingly there was almost no dependence in the drop of the first peak or the characteristics of the time evolution found on the family of the perturbed coupling. This shows that the role of the beyond nearest neighbor interactions in QST is as significant as that of NN couplings.

Using the required number of pulses to have the first peak in fidelity above 0.95 as the measure of how difficult it is to correct for each perturbation for the same scaling factor c and the same network, the most difficult to correct is the change of a single coupling, followed by weakening of all of a qubit's couplings, then change in the magnetic field, and finally the strengthening of all of a qubit's couplings.

In general all of the perturbations we have considered had more pronounced effects on shorter networks than on their larger counterparts and perturbations close to the ends of the chains had more severe effects than those in the middle. We have always

experimented with a varying number of qubits in the network and the other parameters of the protocols such as α and β for the NNN chains in order to check the effectiveness of the Dynamical Decoupling schemes.

It is possible that there are schemes which involve a lower number of operators than those found as well as schemes which eliminate the perturbation to more than the lowest order. However, based on past experiences, the schemes found by the presented algorithm are known to produce applicable schemes [46]. One of the most important aspects of a QST protocol is the time it takes for the transfer to occur. Employing linear programming in a way which minimizes the scaling factor D guarantees minimal arrival time. Additionally, based on simulations, the required numbers of pulses (thousands per second) are within experimental possibilities [26] and therefore realistically applicable.

Chapter 6

Concluding Remarks

Various methods and approaches to realize QST in a simple yet realistic and hence possibly useful protocol of quantum information processing have been found over the years. We chose a framework general enough to demonstrate and work with several of them and hopefully underline the differences between them. The analogy with angular momentum operators allows one to solve easily the Schrödinger equation in the special case of the Krawtchouk chain (2.20), which was the second QST protocol to be discovered [3, 4]. The angular momentum analogy however stops short before giving a method of engineering other QST protocols. On the other hand, the chapters devoted to finding Hamiltonians which generate permutations of the computational basis (3.15) showed how one can find infinitely many Hamiltonians with the QST property. Nevertheless we only worked on linear chains of qubits. Working on graphs has then allowed us to demonstrate how the topological character influences the QST property of the networks and we commented on the first beyond nearest neighbor QST Hamiltonians. We were then able to show most of the known properties of QST Hamiltonians using orthogonal polynomials when we found the necessary and sufficient conditions for Hamiltonians having the QST property and gave another method of engineering infinitely many of them. We employed the orthogonal polynomials to arrive to new results when we showed how to use them to engineer quantum networks on a two dimensional lattice and took a look at constructing QST chains by joining them together.

The infringing considerations we placed upon various QST networks were inspired by realistic conditions stemming from the relationship of the models to the actual underlying physical systems. Both the study of effects of the perturbations on the performance of the networks and the error correcting algorithms are novel results [7, 30]. In order to correct for the perturbations we proposed to somewhat relax the minimal control often

encountered in QST. We needed to assume the possibility of individual qubit control sufficient to apply the Pauli operators. However, these single qubit unitary operations have already been demonstrated experimentally on the very same systems that QST has [16, 17, 18, 19, 28] and therefore the methods presented here should pose no additional requirements on the experimental setups.

The method used — Dynamical Decoupling — has a serious limitation when considered as a tool to modify the performance of a transfer scheme. It cannot create an interaction between the constituents which is not already present in the original system. It is only capable of correcting any existing interaction i.e. decrease its strength in respect to others. Hence the transfer times become longer. In such a case there always exist infinitely many solutions to the main condition (3.10). Comparing the schemes which weaken interactions to those that strengthen interactions in respect to others, we have found the former to be simpler than the latter in the following sense. Schemes which weaken interactions tend to involve a lower number of different operators and for the same performance usually require a lower number of pulses per second. Intuitively the reason for this can be found in the scaling of time. In order to correct for an interaction too strong, the schemes usually only weaken the one interaction while leaving the rest untouched. This scales the time evolution only marginally, we have even seen cases such as (5.13) which are corrected for with no time scaling at all. On the other hand if some of the coupling constants are too weak, Dynamical Decoupling essentially weakens all of the remaining interactions to restore the QST property and this leads to noticeable scaling in time. The scaling in time and the control required for single qubit Pauli operations make up the cost of correcting for the perturbations in the proposed method and can be the basis of a cost function used to quantify the price of correction.

Based on our simulations, the number of required pulses sometimes grew quite large with the size of the system and could pose a severe obstacle for practical setups. Note however that most of the decoupling schemes contain large numbers of the identity operators which amount to doing nothing at all, this alone could bring the number of actually required nontrivial pulses back down to experimentally tolerable numbers. The known experimental setups are capable of applying up to tens of thousands of pulses per π seconds [26], therefore in the most difficult cases we have reached the upper bound on the number of required pulses and stayed well below it otherwise. Further more in chapter 5.1.3 we show that in some cases it is possible to take advantage of the freedom of choosing the solutions to the system of equations (3.26) so that the potentially difficult operations are eliminated from the scheme altogether.

One of the important aspects of QST is the arrival time. For all the protocols

we gave well defined times of arrival. The effect of some of the perturbations was most pronounced in the arrival time. Sometimes the peaks in fidelity did drop, but additionally they shifted in time, became erratic or considerably narrowed. Having a longer read out time at a well defined moment is naturally preferable. Thus the ability to give well defined arrival times once the Dynamical Decoupling schemes are applied can be of significant importance.

Continuing the explorations of both the QST and imperfect quantum networks can enrich our knowledge on quantum state manipulation (QST is a special example), extend its applicability to new systems and make it a reliable elementary building blocks of a functional quantum computer [56]. Many open questions remain. It is an open question to what extend QST should be discussed beyond say one or two dimensions. For the implementation of a quantum computer a two-dimensional structure might be complex enough. However we can deal with other systems. The discussion of transport and specifically QST on graphs is an active field of research and is not reducible to cases in one or two dimensions. In higher dimension and sufficient connectivity among its constituents we have a simple solution of PST at hand. We can guide the excitation (using some decoupling scheme) to the desired target by removing all the interactions except those along a simple linear chain while modifying the remaining ones accordingly. This is a brute force method which works but requires quite a high degree of control on the system and many operations to be applied. However "more" elegant means without so much external control would be certainly interesting and welcome both from a theoretical point of view as well as experimentally.

One of the most recent results is the mapping of QST on the Krawtchouk chain to the continuous time quantum walk on the hypercube. At first this seems like a theoretical niche, but since quantum walks have been demonstrated experimentally repeatedly, this and similar results could open a new path to demonstrations and implementing of QST in many different systems and become a standard for more advanced protocols. The implementation of known protocols on new physical systems is usually just the first step in exploring the potential of such a system. It will require a rethinking of the known approaches to respect and take advantage of all the features new implementation offer.

We saw that the freedom in constructing the decoupling schemes allowed us to tailor them to specific needs such as eliminating all of the σ_z pulses. With new systems being proposed for the demonstration of QST, new correction schemes might be needed since the physical reality of these systems can lead to different restrictions. Additionally, the response of many more QST protocols to perturbations has not been explored yet. For such QST protocols new decoupling schemes could also be found and optimized. We

also saw that different decoupling schemes for QST perform differently and while we gave one generic algorithm for finding such schemes with minimal possible increase in the QST time, other algorithms could be found which would guarantee the efficiency of the resulting decoupling schemes but might perform differently when efficiency and transfer time are evaluated.

Bibliography

[1] Georgios M. Nikolopoulos and Igor Jex. *Quantum State Transfer and Network Engineering*. Quantum Science and Technology. Springer Berlin Heidelberg, 2013.

[2] Sougato Bose. Quantum communication through an unmodulated spin chain. *Physical Review Letters*, 91(20):207901, 2003.

[3] Georgios M. Nikolopoulos, David Petrosyan, and Peter Lambropoulos. Electron wavepacket propagation in a chain of coupled quantum dots. *Journal of Physics: Condensed Matter*, 16(28):4991, 2004.

[4] Matthias Christandl, Nilanjana Datta, Artur Ekert, and Andrew J. Landahl. Perfect state transfer in quantum spin networks. *Physical Review Letters*, 92(18):187902, 2004.

[5] Alastair Kay. A review of perfect state transfer and its application as a constructive tool. *arXiv e-prints*, page arXiv:0903.4274, 2009.

[6] Hiroshi Miki, Satoshi Tsujimoto, Luc Vinet, and Alexei Zhedanov. Quantum-state transfer in a two-dimensional regular spin lattice of triangular shape. *Physical Review A*, 85(6):062306, 2012.

[7] Holger Frydrych, Antonín Hoskovec, Igor Jex, and Gernot Alber. Selective dynamical decoupling for quantum state transfer. *Journal of Physics B: Atomic, Molecular and Optical Physics*, 48(2):025501, 2014.

[8] Luc Vinet and Alexei Zhedanov. How to construct spin chains with perfect state transfer. *Physical Review A*, 85(1):012323, 2012.

[9] Vojtěch Košťák, Georgios M. Nikolopoulos, and Igor Jex. Perfect state transfer in networks of arbitrary topology and coupling configuration. *Physical Review A*, 75:042319, 2007.

[10] Matthias Christandl, Luc Vinet, and Alexei Zhedanov. Analytic next-to-nearest-neighbor xx models with perfect state transfer and fractional revival. *Physical Review A*, 96:032335, 2017.

[11] Georgios M. Nikolopoulos, Antonín Hoskovec, and Igor Jex. Analysis and minimization of bending losses in discrete quantum networks. *Physical Review A*, 85(6):062319, 2012.

[12] David Petrosyan, Georgios M. Nikolopoulos, and P. Lambropoulos. State transfer in static and dynamic spin chains with disorder. *Physical Review A*, 81(4):042307, 2010.

[13] Chris Godsil. State transfer on graphs. *Discrete Mathematics*, 312(1):129–147, 2012.

[14] Hiroshi Miki, Satoshi Tsujimoto, and Luc Vinet. Spin chains, graphs and state revival. *arXiv e-prints*, page arXiv:1903.00145, 2019.

[15] Steven J. Large, Michael S. Underwood, and David L. Feder. Perfect quantum state transfer of hard-core bosons on weighted path graphs. *Physical Review A*, 91:032319, 2015.

[16] Jingfu Zhang, Xinhua Peng, and Dieter Suter. Speedup of quantum-state transfer by three-qubit interactions: Implementation by nuclear magnetic resonance. *Physical Review A*, 73(6):062325, 2006.

[17] Paola Cappellaro, Chandrasekhar Ramanathan, and David G. Cory. Dynamics and control of a quasi-one-dimensional spin system. *Physical Review A*, 76:032317, 2007.

[18] Paola Cappellaro, Chandrasekhar Ramanathan, and David G. Cory. Simulations of information transport in spin chains. *Physical Review Letters*, 99(25):250506, 2007.

[19] Zoltán L. Mádi, Bernhard Brutscher, Thomas Schulte-Herbrüggen, Rafael Brüschweiler, and Richard R. Ernst. Time-resolved observation of spin waves in a linear chain of nuclear spins. *Chemical physics letters*, 268(3-4):300–305, 1997.

[20] Matthieu Bellec, Georgios M. Nikolopoulos, and Stelios Tzortzakis. Faithful communication hamiltonian in photonic lattices. *Optics letters*, 37(21):4504–4506, 2012.

[21] Leo P. Kouwenhoven, Charles M. Marcus, Paul L. McEuen, Seigo Tarucha, Robert M. Westervelt, and Ned S. Wingreen. Electron transport in quantum dots. In *Mesoscopic electron transport*, pages 105–214. Springer Netherlands, 1997.

[22] Sylvain Hermelin, Shintaro Takada, Michihisa Yamamoto, Seigo Tarucha, Andreas D. Wieck, Laurent Saminadayar, Christopher Bäuerle, and Tristan Meunier. Electrons surfing on a sound wave as a platform for quantum optics with flying electrons. *Nature*, 477(7365):435, 2011.

[23] Jonathan P. Home, David Hanneke, John D. Jost, Jason M. Amini, Dietrich Leibfried, and David J. Wineland. Complete methods set for scalable ion trap quantum information processing. *Science*, 325(5945):1227–1230, 2009.

[24] Jonathan Simon, Waseem S. Bakr, Ruichao Ma, M. Eric Tai, Philipp M. Preiss, and Markus Greiner. Quantum simulation of antiferromagnetic spin chains in an optical lattice. *Nature*, 472(7343):307, 2011.

[25] Georgios M. Nikolopoulos, Thomas Brougham, Antonín Hoskovec, and Igor Jex. Communication in engineered quantum networks. In *Quantum State Transfer and Network Engineering*, Quantum Science and Technology, pages 39–86. Springer Berlin Heidelberg, 2013.

[26] Michael J. Biercuk, Hermann Uys, Aaron P. VanDevender, Nobuyasu Shiga, Wayne M. Itano, and John J. Bollinger. Optimized dynamical decoupling in a model quantum memory. *Nature*, 458(7241):996, 2009.

[27] Elliott Fraval, Matthew J. Sellars, and Jevon J. Longdell. Dynamic decoherence control of a solid-state nuclear-quadrupole qubit. *Physical Review Letters*, 95(3):030506, 2005.

[28] John J. L. Morton, Alexei M. Tyryshkin, Arzhang Ardavan, Simon C. Benjamin, Kyriakos Porfyrakis, Stephen Aplin Lyon, and G. Andrew D. Briggs. Bang–bang control of fullerene qubits using ultrafast phase gates. *Nature Physics*, 2(1):40, 2006.

[29] Lorenza Viola and Seth Lloyd. Dynamical suppression of decoherence in two-state quantum systems. *Physival Review A*, 58:2733–2744, 1998.

[30] Antonín Hoskovec and Igor Jex. Dynamical decoupling and NNN discrete quantum networks. *Quantum information & computation*, to be submitted.

[31] Bruce W. Shore and Richard J. Cook. Coherent dynamics of n-level atoms and molecules. IV. two- and three-level behavior. *Physical Review A*, 20:1958–1964, 1979.

[32] David J. Griffiths and Darrell F. Schroeter. *Introduction to Quantum Mechanics*. Cambridge University Press, 2018.

[33] Thomas Brougham, Georgios M Nikolopoulos, and Igor Jex. Communication in quantum networks of logical bus topology. *Physical Review A*, 80(5):052325, 2009.

[34] John Brown, Chris Godsil, Devlin Mallory, Abigail Raz, and Christino Tamon. Perfect state transfer on signed graphs. *arXiv e-prints*, page arXiv:1211.0505, 2012.

[35] Daniel Reitzner, Daniel Nagaj, and Vladimír Bužek. Quantum walks. *Acta Physica Slovaca*, 61(6):603–725, 2011.

[36] Julia Kempe. Quantum random walks: an introductory overview. *Contemporary Physics*, 44(4):307–327, 2003.

[37] Lu-Ming Duan and Guang-Can Guo. Preserving coherence in quantum computation by pairing quantum bits. *Physical Review Letters*, 79(10):1953, 1997.

[38] Peter W. Shor. Scheme for reducing decoherence in quantum computer memory. *Physical review A*, 52(4):R2493, 1995.

[39] Paolo Facchi, Daniel A. Lidar, and Saverio Pascazio. Unification of dynamical decoupling and the quantum Zeno effect. *Physical Review A*, 69(3):032314, 2004.

[40] Wilhelm Magnus. On the exponential solution of differential equations for a linear operator. *Communications on pure and applied mathematics*, 7(4):649–673, 1954.

[41] Douglas P. Burum. Magnus expansion generator. *Physical Review B*, 24:3684–3692, 1981.

[42] James J. Sylvester. LX. thoughts on inverse orthogonal matrices, simultaneous signsuccessions, and tessellated pavements in two or more colours, with applications to Newton's rule, ornamental tile-work, and the theory of numbers. *The London, Edinburgh, and Dublin Philosophical Magazine and Journal of Science*, 34(232):461–475, 1867.

[43] Haralambos Evangelaras, Christos Koukouvinos, and Jennifer Seberry. Applications of hadamard matrices. *Journal of telecommunications and information technology*, 2:3–10, 2003.

[44] Katta G. Murty. *Linear programming*. John Wiley & Sons, 1983.

[45] Dimitris Alevras and Manfred W. Padberg. *Linear Optimization and Extensions: Problems and Solutions*. Springer Berlin Heidelberg, 2012.

[46] Holger Frydrych, Gernot Alber, and Pavel Bažant. Constructing Pauli pulse schemes for decoupling and quantum simulation. *Physical Review A*, 89:022320, 2014.

[47] Theodore S. Chihara. *An Introduction to Orthogonal Polynomials*. Gordon and Breach, 1978.

[48] Feliks R. Gantmakher and Mark G. Krejn. *Oscillation matrices and kernels and small vibrations of mechanical systems*. AMS Chelsea Publishing: An Imprint of the American Mathematical Society, 2002.

[49] Graham M. L. Gladwell. Inverse problems in vibration. *Applied Mechanics Reviews*, 39(7):1013–1018, 1986.

[50] Luc Vinet and Alexei Zhedanov. A characterization of classical and semiclassical orthogonal polynomials from their dual polynomials. *Journal of computational and applied mathematics*, 172(1):41–48, 2004.

[51] Chi-Kwong Li and Ren-Cang Li. A note on eigenvalues of perturbed hermitian matrices. *Linear algebra and its applications*, 395:183–190, 2005.

[52] Gilbert W. Stewart and Ji-guang Sun. *Matrix Perturbation Theory*. Computer science and scientific computing. Academic Press, 1990.

[53] Roger Fletcher. *Practical methods of optimization*. Wiley Online Library, 1987.

[54] Joaquin Bustoz, Mourad E. H. Ismail, and Sergei Suslov. *Special functions 2000: current perspective and future directions*, volume 30. Springer Science Ḅusiness Media, 2012.

[55] Alberto F. Grünbaum and Mizan Rahman. On a family of 2-variable orthogonal Krawtchouk polynomials. *SIGMA. Symmetry, Integrability and Geometry: Methods and Applications*, 6:090, 2010.

[56] David P. DiVincenzo. The physical implementation of quantum computation. *Fortschritte der Physik: Progress of Physics*, 48(9-11):771–783, 2000.

[57] Alastair Kay. The basics of perfect communication through quantum networks. *Physical Review A*, 84:022337, 2011.